AN ABSTRACT OF THE THESIS OF

Bailey J. Dickey for the degree of Master of Science in Pharmacy
presented on August 21, 2015.

Title: Metabolomic Profiling of Natural Products from Two *Tolypocladium* Fungal Species as Part of An Evolutionary Genomics Study

Abstract approved:

_____

Kerry L. McPhail

This thesis describes an investigation of the natural products chemistry of two fungal species of the genus *Tolypocladium*. Natural products are small organic molecules that are considered non-essential for cell growth and reproduction, and thus part of secondary metabolism. Chemical profiling of these secondary metabolites using a combination of high-performance liquid chromatography (HPLC) and mass spectrometry (MS), as well as ^{1}H nuclear magnetic resonance (NMR) spectroscopy, identified a number of known and unknown natural products of *Tolypocladium inflatum* and *T. geodes*. In particular, putative new peptaibols were detected by LC-MS/MS profiling, although these data were insufficient for structural characterization. To determine the effect of a putative secondary metabolite regulator, comparative metabolomic profiling was performed of *T. inflatum* wild-type and a knockout mutant in which the genes for a homolog of the histone methyltransferase KMT6 had been deleted. A preliminary result on the deletion of the kmt6 gene homolog suggests a knockdown of CsA and possibly the putative new peptaibols. Finally, to demonstrate the potential of *T. inflatum* to produce medicinally-relevant molecules with new biological activities, extracts and fractions were screened against the human pathogen *Neisseria gonorrhoeae*. Some test samples appeared to possess potent activity and, suggesting that they contain compounds, which inhibit the growth of *N. gonorrhoeae*.

Metabolomic Profiling of Natural Products from Two *Tolypocladium* Fungal Species as Part of An Evolutionary Genomics Study

by
Bailey J. Dickey

A THESIS

submitted to

Oregon State University

in partial fulfillment of
the requirements for the
degree of

Master of Science

Presented August 21, 2015
Commencement June 2016

Master of Science thesis of Bailey J. Dickey presented on August 21, 2015

APPROVED:

Major Professor, representing Pharmacy

Dean of the College of Pharmacy

Dean of the Graduate School

I understand that my thesis will become part of the permanent collection of Oregon State University libraries. My signature below authorizes release of my thesis to any reader upon request.

Bailey J. Dickey, Author

ACKNOWLEDGEMENTS

Firstly, I would like to thank my family. The tri-generation trio: my grandfather, father and brother who have always been very supportive throughout my graduate career. They have helped me to reach my full potential and to achieve the best. As well as my mother, the best storyteller who articulates detailed descriptions of her travels, reminding me that life is full of adventure. My grandmother Bonnie, a strong hearted women with a great sense of humor that has gave me the courage to strive for a career in the sciences and to never give up using the phrase," It's not over until the heavy lady sings"! A big thank you also goes to my dog Bebe for always being their by my side, quite literally. Most of all however, to my boyfriend who has pushed me to do my best, been there through the tough times and taught me that a cup of tea solves everything.

I would also like to thank Dr. Kerry McPhail for giving me the opportunity to come to OSU. She has been a great source for guidance and I truly appreciate all her help throughout my project. I would also like to extend my gratitude to Dr. Joey Spatafora and Rheannon Arvidson for their support and all the genomic work that was contributed to the project as well as, Dr. Sandra Loesgen, Dr. Taifo Mahmud, Dr. Benjamin Philmus and Dr. Patrick Videau who have also proven useful sources of conversation and mentorship through the course of my masters degree. I would also like to thank funding provided by the National Science Foundation.

Lastly, to my lab mates and friends Igor, Dorota and Arun who have put up with me for the past two years and have been the best roommates I could ask for.

CONTRIBUTION OF AUTHORS

The Spatafora Lab provided all *Tolypocladium* species and all the phylogenetic studies, with contributions from Dr. Joey Spatafora, Rheannon Arvidson, Dr. Alisha Quandt and Dr. Kathryn Bushley. Dr. Kerry McPhail contributed throughout the metabolomic profiling of *Tolypocladium* as well as, previous work contributed from Mariko Nonogaki. Additionally, the Sikora Lab performed the *Neisseria gonorrhoeae* growth inhibitory assay contributed from Dr. Alexandra Sikora and Igor Wierzbicki.

TABLE OF CONTENTS

Page

CHAPTER ONE: General Introduction..... 1

Natural Products and their Role in Human Health and Agriculture 2

Historically Important Fungal Natural Products.....3

Metabolomic Profiling as a means of isolating Fungal Natural Products.....6

Overview of the Evolutionary Biology of the Fungal Order Hypocreales.....11

Inter and intra-kingdom host shifts within the Hypocreales……..…….....12

Known Secondary Metabolites of *Tolypocladium*.....13

Project Aims.....20

CHAPTER TWO Metabolomic profiling of *Tolypocladium inflatum and T.* geodes.....22

Introduction..... 23

Methods and Materials..... 24

Results and Discussion 27

Conclusion 44

CHAPTER THREE:

Loss of cyclosporin A Production in a Genetic Knockout of a *kmt6* methyltransferase homolog in *T.* inflatum.....46

Introduction..... 47

Methods and Materials.....51

Results and Discussion 56

Conclusion.....69

Bibliography 72

LIST OF FIGURES

Figure Page

Figure 1.1 Structures of penicillin G, cephalosporin C, fusidic acid griseofulvin, and mevinolin 4

Figure 1.2 Structures of fusarisetin A and macrosphelide B 5

Figure 1.3 An example of metabolomics profiling taken from Müller et al. in the discovery of myxoprincomide 8

Figure 1.4 Structures of chlorinated (top) and brominated (bottom) anthraquinones with numbering scheme designating the name 9

Figure 1.5 Structure of fellutamide B 10

Figure 1.6 Phylogeny of Hypocreales 13

Figure 1.7 Structure of cylosporin A 15

Figure 1.8 Structure of FR190293 16

Figure 1.9 Structure of efrapeptin D 17

Figure 1.10 Structures of the peptaibols LP237-F5, -F7, and -F8 18

Figure 1.11 Structures of fumonisins B2 and B4 19

Figure 1.12 Structure of tolypoalbin 19

Figure 2.1 LC-MS spectrum of putative peptaibols from *T. inflatum* 24

Figure 2.2 Diagram of reverse phase extraction method 25

Figure 2.3 LC-MS/MS spectrum of putative peptaibols in PDB 29

Figure 2.4 LC-MS/MS spectrum of putative peptaibols in SM 30

Figure 2.5 LC-MS/MS spectrum of *T. inflatum* cultured in SM showing CsA. 32

Figure 2.6 LC-MS/MS spectrum of *T. geodes* cultured on PDA showing CsA 33

Figure 2.7 Metabolomic profiling identified known fumonisins in the organic extract of *T. inflatum* 34

LIST OF FIGURES CONTINUED

Figure Page

Figure 2.8 Metabolomic profiling identified fumonisins not previously known to be reported with *T. inflatum*..... 35

Figure 2.9 Metabolomic profiling identified efrapeptines G and F, known to be reported with *T. geodes*..... 36

Figure 2.10 HPLC trace depicting fractionation of 100% MeOH fraction Ti8044-PDB-M.....37

Figure 2.11 Metabolomic profiling identified CsA in fraction C from the HPLC trace of Ti8044-PDB-M and LC-MS spectra of standard CsA 38

Figure 2.12 H^1 NMR spectra of CsA standard in $CDCl_3$ at 500 MHz.....39

Figure 2.13 Comparision of the CsA stanadard and the CsA isolated from fraction C.....40

Figure 2.14 Metabolomic profiling identified putative peptaibol 5 and CsA in fraction B4 from the HPLC trace of Ti8044-PDB-M 41

Figure 2.15 Metabolomic profiling identified putative peptaibol 3 and CsA in fraction Co from the HPLC trace of Ti8044-PDB-M. 42

Figure 2.16 Metabolomic profiling identified fumonisin B2 and PHFB2c in fraction B0 from the HPLC trace of Ti8044-PDB-M 43

Figure 2.17 Mass spectrometry heat map of the metabolites found in the extract of T-8044-PDB-M..... 45

Figure 3.1 Structure of nucleosome 48

Figure 3.2 An illustration depicting H3 histone modification from Sada/Ada complex and LaeA 49

Figure 3.3 A chemical reaction mechanisum describing histone methylation modifications of lysine residues..... 50

Figure 3.4 LC-MS spectrum of *T. inflatum* extracts from 100% MeOH fraction using reverse phase extraction method displaying metabolite similarities..... 58

LIST OF FIGURES CONTINUED

Figure Page

Figure 3.5 LC-MS data for the 100% MeOH fractions of *T. inflatum* extracts grown in PDB showing the loss of reproducibility from the original sample.....59

Figure 3.6 LC-MS spectrum of TIC normal phase extracted fractions, F and E from *T. inflatum* showing suspected cyclosporin masses.....60

Figure 3.7 LC-MS spectrum of TIC normal phase extracted fractions, G showing putative peptaibol masses 61

Figure 3.8 LC-MS spectrum of *T. inflatum* extracts from 100% MeOH fraction using reverse phase extraction method displaying metabolite differences.....63

Figure 3.9 LC-MS spectrum of the reverse phase extracted 100% MeOH fraction from *T. inflatum* diplaying loss of cyclosporin A in the KO.....64

Figure 3.10 A chart displaying the OD_{600} readings of GC growth in the presence of the *T. inflatum* extracts over 9 hours.....66

Figure 3.11 HPLC trace of the 100% MeOH from the extract TiKO-D6-6-Or-MeOH depicting further fractionation.....68

Figure 3.12 A chart displaying the OD_{600} readings of GC growth in the presence of the *T. inflatum* extracts over 9 hours.....68

LIST OF TABLES

Table Page

Table 1.1 Sequences of efrapeptins C-J from *Tolypocladium* species …….....…….....17

Table 3.1 A list of reverse phase extracted fractions from *T. inflatum* WT/KO aqueous and organic extracts in PDB for the day course study.....52

Table 3.2 A list of the reverse phase extracted fractions from *T. inflatum* WT/KO organic extracts in SM for media study …….....….....53

Table 3.3 A List of the normal phase extracted fractions from *T. inflatum* in PDB.....55

Table 3.4 A list of the percent mass yields from the extracts listed in table 3.1 of the day course study…….....…….....57

Table 3.5 A list of the percent mass yields from the extracts listed in table 3.2.....60

LIST OF ABBREVIATIONS

A-domain	adenylation domain
Abu	2-aminobutyric acid
Ac	acetyl
ACN	acetonitrile
ACV	δ-($_{L}$-α-aminoadipyl)-L-cystine-D-valine
Aib	α-aminoisobutyric acid
Ala	alanine
Aq	aqueous
ATPases	adenosine triphosphatase
Bmt	butenyl-methyl-L-threonine
C	celsius
CsA	cyclosporin
CyP	cyclophilin
Da	daltons
DCM	dichloromethane
DMSO	dimethylsulfoxide
DNA	deoxyribose nucleic acid
ESI	electrospray ionization
EtNor	α-ethylnorvaline
EtOAc	ethyl acetate
FA	formic acid
G	grams
GC	*Neisseria gonorrhoeae*
GCBL	gonococcal base liquid
h	hour
HDAC	histone deacetylases
HIV	human immunodeficiency virus
HPLC	high performance liquid chromatography
IC_{50}	50% inhibitory concentration
Iva	L-iso-valine
KMT	lysine methyltransferase
KO	knockout
L	liter
LC-HRMS	liquid chromatography high resolution mass spectrometry
LC-MS	liquid chromatography resolution mass spectrometry
LD_{50}	50% Lethal Dose
Leu	leucine
LOL	leucinol
LR-LCMS	liquid chromatography low resolution mass spectrometry
m	milli
Me	methyl

MeOH	methanol
MHz	mega hertz
Min	minutes
MS	mass spectrometry
MS/MS	mass spectrometry mass spectrometry
NF-AT	nuclear factor of activated T-cells
Nm	nanometer
NMR	nuclear magnetic resonance
NP	natural product
NRPS	non-ribosomal peptide synthases
OD_{600}	optical density
Or	organic
PCA	principal component analysis
PDA	potato dextrose agar
PDB	potato dextrose broth
PKS	polyketide synthetase
Ppm	parts per million
RNA	ribonucleic acid
RP	reverse phase
rpm	revolutions per minute
RT	retention time or room temperature
SAHA	suberanilohydroxamic acid
SAM	*S*-adenosylmethionine
Sar	sarcosine
SM	secondary metabolite or synthetic media
SPE	solid phase extraction
STI	sexually transmitted infection
TCA	tricarboxylic acid
TIC	total ion chromatograph
UPLC-PDA-HRMS-MS/MS	ultraperformance liquid chromatography−photodiode array−high-resolution tandem mass spectrometric
UV	ultraviolet
Val	valine
WT	wild type
XIC	extracted ion chromatograph
µ	micro

CHAPTER ONE

General Introduction

Bailey J. Dickey

Natural Products and their Role in Human Health and Agriculture

Natural Products (NPs) are organic compounds that are produced by living organisms such as microbes, plants and fungi, and are generally considered to be part of secondary metabolism. Primary metabolism comprises the general pathways that are common among living organisms, such as glycolysis, tricarboxylic acid cycle and oxidation of fatty acids. Secondary metabolism, unlike primary metabolism, is nonessential to the growth and reproduction of the organism, at least under the conditions studied, and constitutes a biosynthetic system in which enzymes catalyze a sequence of specific reactions to produce secondary metabolites (SM). Secondary metabolites (SM) are generally restricted to taxonomic groups of organisms and have diverse, unique and often complex structures with biological activity. For example, members of the Phylum Ascomycota produce beta lactam antibiotics, the penicillins and cephalosporins, using a multifunctional enzyme that is transcribed by DNA, and synthesizes peptides for which the genetic sequence is not coded within the genome. These enzymes are referred to as non-ribosomal peptide synthetases (NRPS). The biosynthesis of tripeptide penicillin G, for example, is accomplished by the NRPS, δ-($_{L}$-α-aminoadipyl)-L-cysteinyl-D-valine (ACV synthetase). Secondary metabolites serve as an excellent source of lead compounds for drug development due to their diverse structures and intricate carbon skeletons. These scaffolds are often referred to as "privileged" based on the fact that chemical entities produced by living organisms have evolved under selection pressure and are therefore more likely to have a specific biological activity. In 2003, Feher & Schmidt, computationally analyzed the differences between natural products and libraries of synthetic and combinatorial compounds by their chemical diversity and "drug-likeness". The workers defined

"drug-likeness" as features that are shared by other molecules currently utilized as drugs. The work showed that an increase in stereogenic centers in natural products correlates with better stereo-specificity for biological targets and therefore a greater binding affinity for their particular targets. In a 2012 review, Newman & Cragg, assessed the sources of new drugs over the last 30 years. The authors showed that the vast majority of approved drugs are compounds derived from natural products. It was also stated that only one *de novo* drug, sorafenib (Nexavar®) for renal cell and hepatocellular carcinoma, has been approved by the FDA. Sorafenib was discovered by assembling and screening a combinatorial (synthetic) compound library, an approach often utilized by the pharmaceutical industry.

Historically Important Fungal Natural Products

Fungi have been shown to produce a wide range of natural products that are used throughout the pharmaceutical industry. Perhaps the most famous and most significant of these discoveries were of the antibiotics penicillin and cephalosporin. Alexander Flemings first discovered penicillin in 1928 from the ascomycete *Penicillium rubens* (Order Eurotiales); cephalosporin was isolated from *Cephalosporium acremonium* by Giu in 1948 [3], and subsequently renamed *Acremonium strictum* (Order Hypocreales). Both penicillin and cephalosporin inhibit cell wall synthesis by irreversibly binding to a transpeptidase, an enzyme that catalyzes peptide bond formation. Without the transpeptidase bacteria are unable to cross-link peptidoglycan strands and as a result are unable to form new cell walls, which ultimately leads to cell death. Godtfredsen et. al, [1962] further demonstrated the potential of fungal natural products as a source for antibiotics. The group isolated the steroid fusidic acid from *Fusidium coccineum*

(Order Hypocreales) [Godtfredsen et. al, 1962]. Fusidic acid blocks protein synthesis by preventing the release of elongation factor G, a GTPase that catalyzes the translocation step during bacterial protein synthesis.[Bodley et. al., 1969]

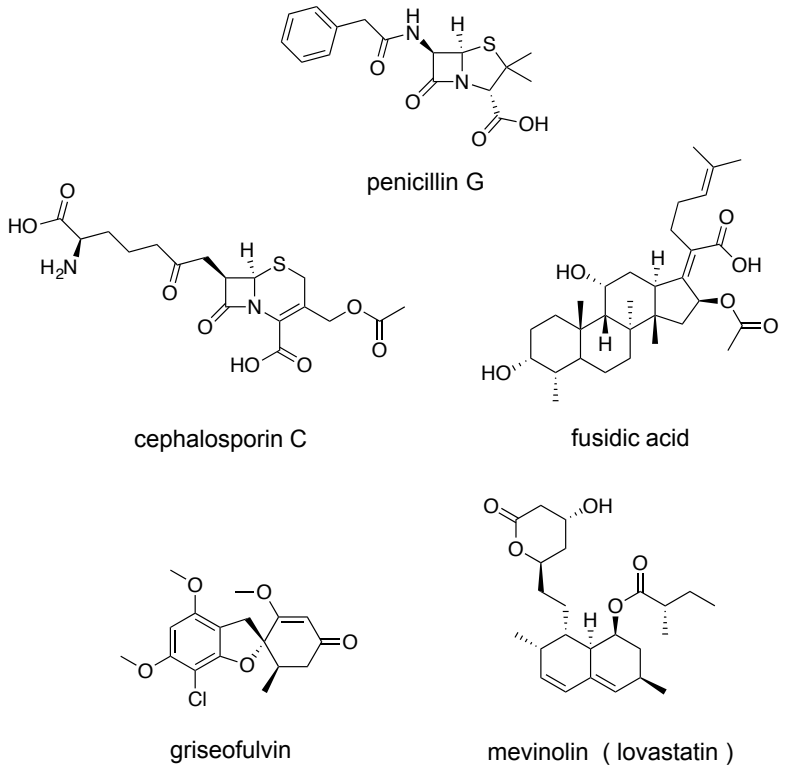

Figure (1.1) Structures of penicillin G, cephalosporin C, fusidic acid griseofulvin, and mevinolin.

It is not only antibacterials that can be found through investigation of fungal metabolites. Griseofulvin isolated from *Penicillium griseofulvum* is an antifungal agent that targets tubulin.[Oxford et al., 1939] This polyketide inhibits mitosis by binding to tubulin, a dimeric cytoskeletal protein that polymerizes into microtubules that form the mitotic spindle.[Weber et al, 1976] Mevinolin is another fungal-derived polyketide, better known as lovastatin, which was discovered by Alberts in 1978 from *Aspergillus terrus*, shortly after the discovery of compactin (mevastatin) by Endo et al. [1976]. These "statins" have been shown to target HMG Co-A reductase, an enzyme

that catalyzes an early step in cholesterol biosynthesis, to lower blood levels of cholesterol. These historical natural products are shown in Figure 1.1.

The immunosuppressant drug cyclosporin A (CsA), together with congeners B-Z, is another historically important fungal metabolite. In the 1970's, a Swiss pharmaceutical company called Sandoz Ltd. (Basel) was searching for an immunosuppressant agent with low cytotoxicity, which led to the discovery of CsA. CsA is a cyclic undecapeptide that contains several unusual amino acids with interesting biological activity and will be discussed further in the following chapters.

A 2014 review from Evidente et al. [2014] reports several fungal NPs with promising anti-cancer activity that are expected to enter human clinical trials in the near future. The latter review demonstrates the structural diversity and potential anticancer properties of fungal NPs by highlighting several examples. These include the *Fusarium sp.* FN080326 metabolite fusarisetin A, a cancer cell migration inhibitor that comprises a unique new pentacyclic carbon skeleton, and macrosphelide B, a 16-membered macrocyclic metabolite from *Periconia bissoides* that suppresses metastasis by preventing loss of cell adhesion (Figure 1.2).

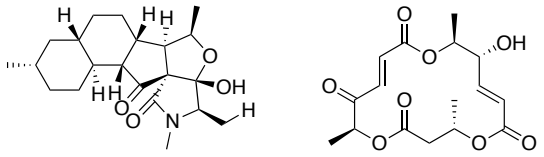

Figure (1.2) Structures of fusarisetin A and macrosphelide B

Mycotoxins are not typically used as therapeutics due to their high cytotoxicity, but are important in agriculture. In the corn maize industry, detection of fumonisins is imperative because of their high hepatotoxicity and carcinogenicity to humans and animals.[Gelderblom et al., 1988][Li et al., 2015] Fumonisins were first discovered from *Fusarium* fungi that naturally contaminate maize.[Gelderblom et al.,1988]. Additionally, fumonisins B1 and B2 inhibit ceramide synthase, which interferes with the function of many membrane proteins.[Marasas et al., 2004] Fumonisins will be further characterized in this chapter and elucidated by MS/MS in Chapter Two.

Fungi have also been investigated in an agricultural setting as biological control agents for plant pathogens. The best known examples are mycoparasitic species of the genus *Trichoderma*. Sriwati et al. [2015] have used *Trichoderma virens* as a biocontrol on the cocoa tree *Theobroma cacao* L., which suffers large yield losses in Aceh, Indonesia due to black pod rot, a disease caused by the oomycetes (water molds) of the genus *Phytophthora*. The mycoparasitic activity of *Trichoderma virens* can be associated with its production of several potent epithiodiketopiperazine antibiotics, including gliotoxin and gliovirin.[Howell et al., 2007]

Metabolomic profiling as a means of identifying fungal natural products

The importance of fungal-derived natural products in medicine has led to significant research efforts over the past 40 years. The most common and successful approach to mining the secondary metabolites of fungi has been through analyzing their metabolomics profiles. Yuliana et al. [2011] define metabolomics as the "systematic study of the metabolites (the metabolome) present in an organism at a specific time

and under specific conditions, and including both qualitative and quantitative analyses". The most common means of undertaking a metabolomic profile is by analyzing the extracts via liquid chromatography and then using a combination of high resolution mass spectrometry (LC-HRMS) and principal component analysis to identify the components of the extract.[Yuliana et al., 2011] Principal component analysis (PCA) is a statistical method that uses clustering or pattern recognition algorithms on large multivariate data to help visualize outliers or trends.[Yuliana et al., 2011] The figure below was adapted from a 2014 review by Krug et al. [2014] and illustrates the metabolomics process using the example of the myxobacterium *Myxococcus xanthus*. Previous bioinformatics analysis revealed 13 unassigned biosynthetic gene clusters encoding NRPS, PKS and hybrid pathways. Knockout mutants were created for these gene clusters and processed in the metabolomics pipeline, leading to the discovery of both a large hybrid peptide-polyketide gene cluster, *mxp* and the biosynthetic product myxoprincomide (Figure 1.3).

A.

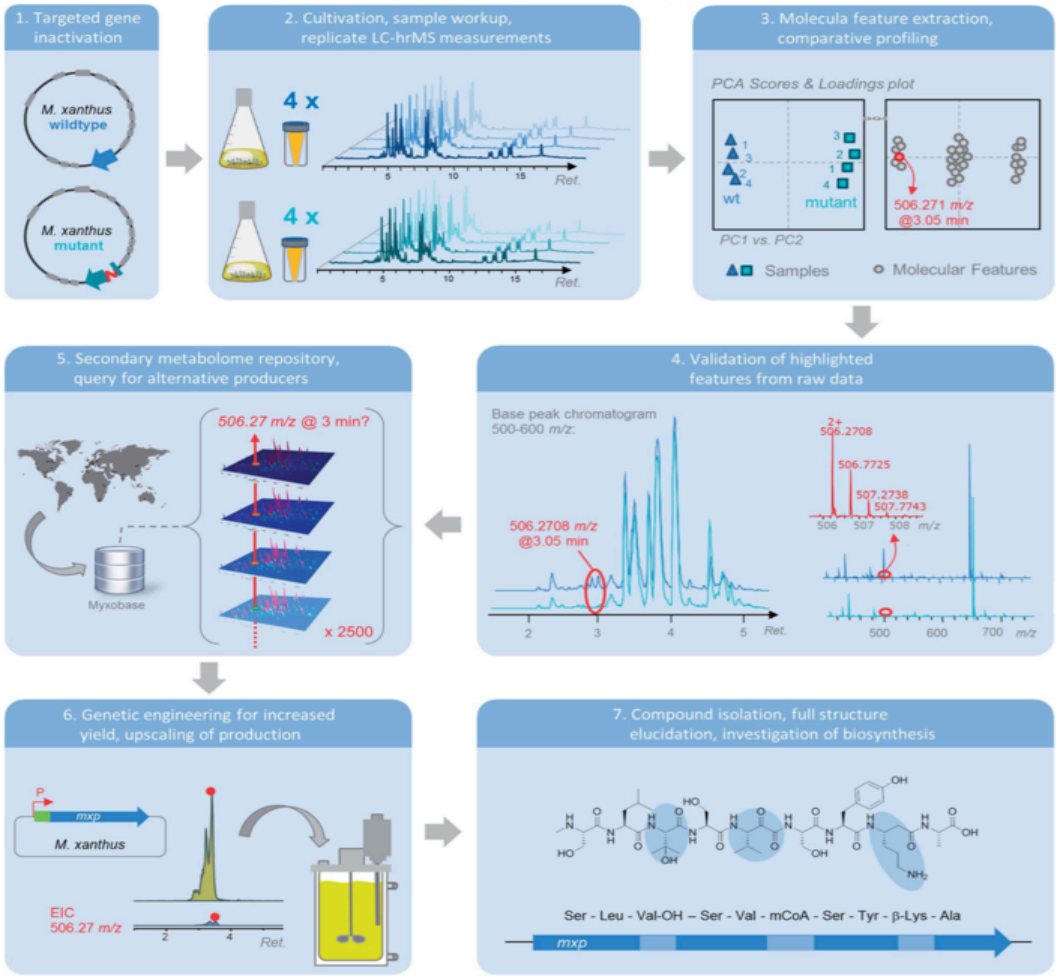

B.

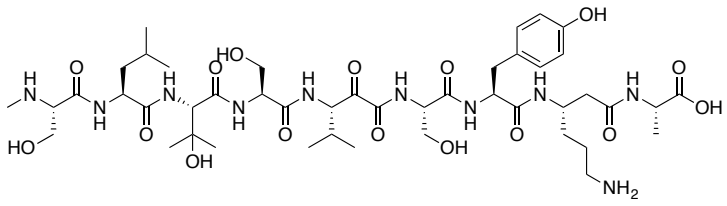

myxoprincomide

Figure (1.3) An example of metabolomics profiling taken from Krug et al. [2014] in the discovery of myxoprincomide. (A) A diagram of the workflow for metabolomics profiling. Replicates of both the wild type and knock out mutants were created and profiled via LC-HRMS. Mass spectrometric data were statistically analyzed using PCA, which reveals the outlier ion *m/z* 506.271 from the wild-type, that is absent from the *mxp* mutant. After validation of the ion from the original chromatogram, repositories were queried for other producers of the same ion. Yields of the unknown product were increased by genetically engineering the *mxp* gene cluster, leading to the elucidation of myxoprincomide, 506.208 = $[M+2H]^{2+}$. (B) Structure of myxoprincomide.

Huang et al. [2012] have used metabolomics profiling to discover a class of chlorinated anthraquinones from marine-derived *Aspergillus sp*. SCSIO F063 (Order Eurotiales). Recognizing that the biosynthetic machinery existed in *Aspergillus sp*. SCSIO F063 to produce these halogenated compounds, the fermentation broth was supplemented with sodium bromide. As anticipated, two new brominated anthraquinones were obtained (Figure 1.4).

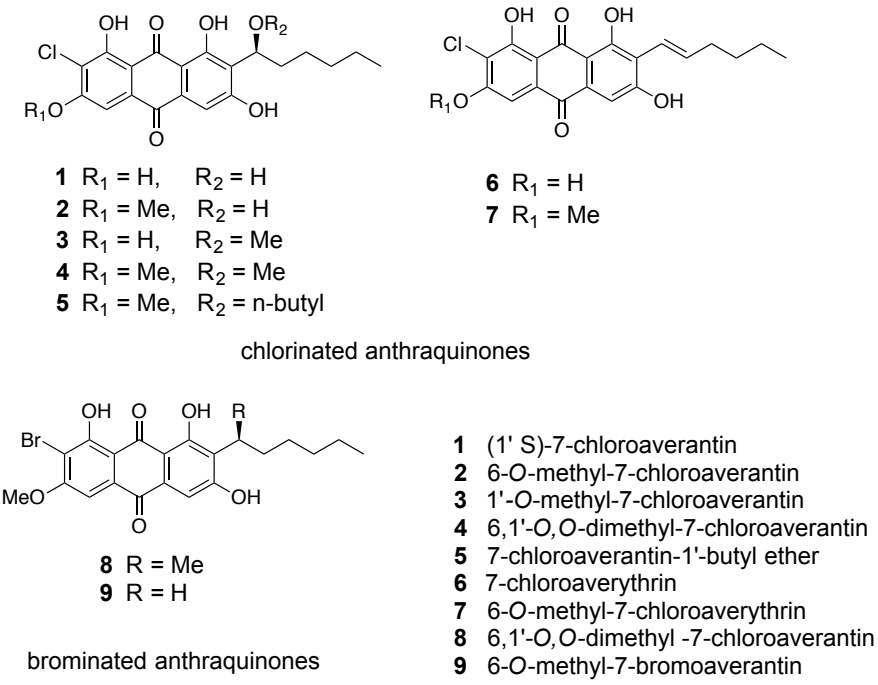

Figure (1.4) Structures of chlorinated (top) and brominated (bottom) anthraquinones with numbering scheme designating the name.

One challenge with traditional natural products discovery is that the approach can often lead to repetitive known chemistry, which in the majority of instances takes a prolonged period of time to deduce. To overcome this, El-Elimat et al. [2013] constructed a high-resolution (HR) MS, MS/MS, and UV Database for the dereplication of known cytotoxic fungal secondary metabolites using an ultraperformance liquid chromatography−photodiode array−high-resolution tandem

mass spectrometric (UPLC-PDA-HRMS-MS/MS) method. Because fungi are well known to produce cytotoxic compounds, such as the aflatoxins, cytotoxicity assays were used to target possible antitumor compounds to be submitted for dereplication.[El-Elimat et al., 2013] Due to the limited amount of dereplication data for fungal secondary metabolites, this database is important for advancing fungal metabolomics and natural products discovery.

In an untargeted, comparative metabolomics approach by Albright et al. [2015] the metabolite production was monitored for *Aspergillus nidulans* grown in the presence and absence of an epigenetic modifier (suberoylanilide hydroxamic acid, SAHA). SAHA inhibits histone deacetylases (HDACs), which are responsible for regulating and removing local chromatin modifications (N-acetyl substituents) that either promote or repress gene transcription.[Albright et al., 2015] Originally found in *Penicillium fellutanum*, fellutamide B was shown for the first time to be produced by *A. nidulans*.[Albright et al., 2015][Shigemori et al., 1991] Fellutamide B contains a 3-hydroxydodecanoic acid and a dl-mixture of 2-amino-4-methylpentanal (leucinal).[Shigemori et al., 1991]

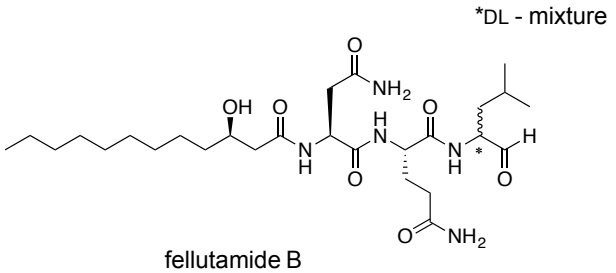

Figure (1.5) Structure of fellutamide B. Both enantiomers of leucinal were isolated (*DL-mixture).

Overview of the Evolutionary Biology of the Fungal Order Hypocreales

In the Kingdom Fungi there are over 700 species within the 100 genera of known entomopathogenic fungi.[Molnár et al., 2010] Since 1968, Savile et al. [1968] have designated pathogenic fungi as either plant-associated, relating them to their preferred plant-host, or as saprobes, which consume dead organic matter, or as animal pathogens, thus introducing the concept of ancestral roots. The evolutionary mechanisms behind this diversification of habitat/ feeding mode remains a central question for mycologists. Microscopic, usually asexual, spores of entomopathogenic fungi have the unique ability to attach to and penetrate insect cuticle, and subsequently colonize and sequester nutrients from insects. The Order Hypocreales comprises the largest number of insect/animal pathogenic species of any fungal order, although it also incorporates a range of fungi associated with plants and other fungi, with life cycles that include anamorphic (asexual), teleomorphic (sexual), or both, reproductive stages.[Kepler et al., 2012][Sung, Hywel-Jones, et al., 2007] The former taxonomy of Hypocreales was largely dictated by morphological characteristics, and previously identified as monophyletic the hypocrealean genus *Cordyceps,* which is a complex group comprising over 400 species of insect and arthropod parasites within the family Clavicipitaceae. [Sung, Hywel-Jones, et al., 2007] However, phylogenetic studies reported by Spatafora et al. [2007] and Sung et al. [2007] present *Cordyceps* as polyphyletic, with multiple ancestral attributes. Therefore, revision of the Hypocreales led to the assignment of three distinct families, Clavicipitaceae, Cordycipitaceae and Ophiocordycipitaceae.[Sung, Hywel-Jones, et al., 2007] The evolutionary history of these families incorporates several inter-kingdom host shifts, which may provide insight into the evolution of entomopathogenic fungi.[Sung et al. 2008]

Clavicipitaceae includes necrotrophs of plants, insects and fungi.[Sung et al., 2008] Additionally, it contains plant pathogens such as the ergot and grass endophytes, which are hypothesized to derive from animal pathogens.[Sung et al., 2008][Spatafora et al., 2007] Cordycipitaceae mainly contains insect pathogens and pathogens of other fungi, with early ancestral lineages that are assumed to comprise symbionts of animals, fungi and plants.[Sung et al., 2008] The Ophiocordycipitaceae family displays very strong intra-species host variation and contains the species that are the focus of this thesis. Ophiocordycipitaceae has the most diverse insect pathogens in Hypocreales, and consists mainly of insect pathogens with ancestral origins of animal parasitism.[Sung et al., 2008][Quandt et al., 2014] The genomic analyses of Spatafora et al. [2007] and Sung et al. [2007] provided a deeper understanding of the taxonomy by contributing detailed phylogenetic data for entomopathogenic fungi in Hypocreales.

Inter and intra-kingdom host shifts within the Hypocreales

Extensive phylogenomic work in the Spatafora Lab has led to better understanding of the phylogeny of the order Hypocreales. The resulting phylogenetic tree for the Hypocreales depicts the preferred nutrient sources among the families (Figure 1.6). The phylogeny of the order Hypocreales has exposed multiple inter-kingdom and intra-family host shifts, with different nutrient sources among families and genera, respectively. There are eight known hypocrealean groups comprising fungi associated with plants, animals and other fungi. In the Ophiocordycipitaceae family, *Tolypocladium inflatum* shows a unique host preference in that it is an insect pathogen of beetle larvae, in contrast to other relatives, which prefer plant or fungal hosts shown in Figure 1.6.

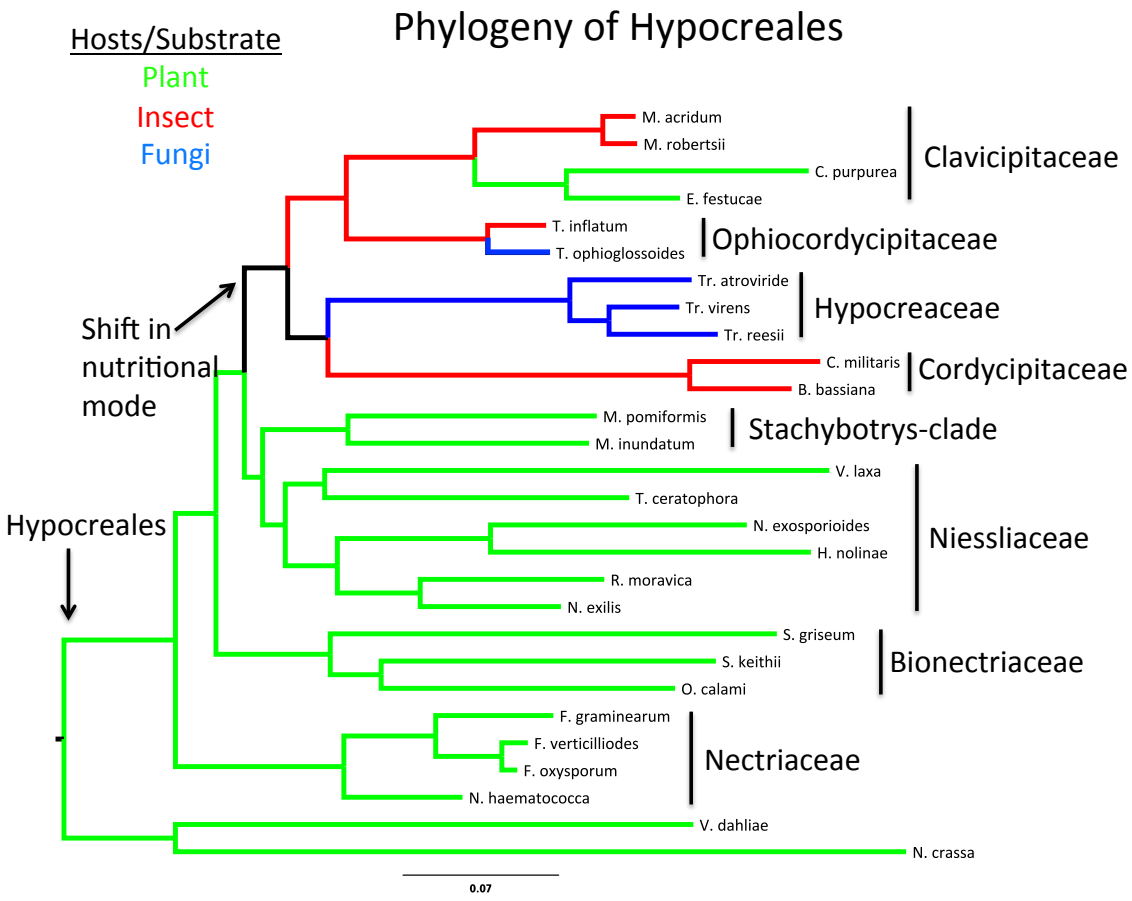

Figure (1.6) Phylogenetic tree for the Hypocreales provided by the Spatafora Lab. Color-coding corresponds to fungal host: green = plant associated, blue = fungal associated, red = animal or insect associated. Hypocreales is delineated at the node shown as "Hypocreales". A major shift from early diverging taxa that have primarily plant-associated hosts to either animal/insect or fungal hosts occurs at the black colored node labeled as "Shift in nutritional mode". Within Family Ophiocordycipitaceae nutritional modes differ between different species of the genus *Tolypocladium*.

Known Secondary Metabolites of *Tolypocladium*

Cyclic Peptides

In *Tolypocladium inflatum* one of the main compounds produced is the immunosuppressant drug, cyclosporin A (CsA).[Borel et al., 1997] CsA is a cyclic undecapeptide that contains the nonproteinogenic amino acids butenyl-methyl-L-threonine (MeBmt), sarcosine (Sar), 2-aminobutyric acid (Abu) and D-alanine (D-Ala). The full sequence of the peptide is MeBmt-Sar-Abu-MeLeu-Val-Ala-[D]Ala-MeLeu-

MeLeu-MeVal with cyclization occurring between the amino group of the D-Ala-8 residue and the carboxylic acid of the Ala-7 residue (Figure 1.7).[Velkov et al., 2011] CsA exerts its immunosuppressant capabilities through inhibition of calcineurin, a calcium-dependent serine/threonine phosphatase. In order to do this CsA must initially bind to the small cytoplasmic protein cyclophilin (CyP), a protein-folding peptidyl-prolyl isomerase.[Pflügl et al., 1993] Binding to cyclophilin occurs on the northern half of CsA through hydrogen bonding and hydrophobic interactions with six residues, MeBmt-1, Abu-2, Sar-3, MeLeu-9, MeLeu-10, and MeVal-11.[Pflügl et al., 1993] The CyP-CsA complex can then bind to calcineurin and prevent induction by dephosphorylation of NF-AT (Nuclear Factor of Activated T-cells), which is a transcription factor responsible for interleukin 2 expression and consequently T-lymphocyte activation.[O'Keefe et al., 1992] It is thought that two key hydrogen bond interactions one between the carbonyl oxygen of Val-5 in CsA to the indole nitrogen of Trp-352 of calcineurin and the amide NH of Ala-7 in CsA to the phenolic OH of Try-341 are the primary cause for disruption of this final protein-protein interaction.[Jin et al., 2002] The gene responsible for the biosynthesis of CsA is the NRPS *simA* and is primarily found within hypocrealean fungi.[Weber et al., 1994] There are 11 modules of the NRPS that are characterized by three core catalytic domains: adenylation (A), which binds and activates the amino acid substrate, thiolation (T), which attaches substrates to the NRPS, and condensation (C), which forms a peptide bond between adjacent substrates. Each substrate is activated by each module with additional methylation (Me) domains that methylate substrates 1 (Bmt), 2 (Abu), 3 (Sar), 4 (Leu), 6 (Leu), 9 (Leu), 10 (Leu), 11 (Val).[Bushley et al., 2013]

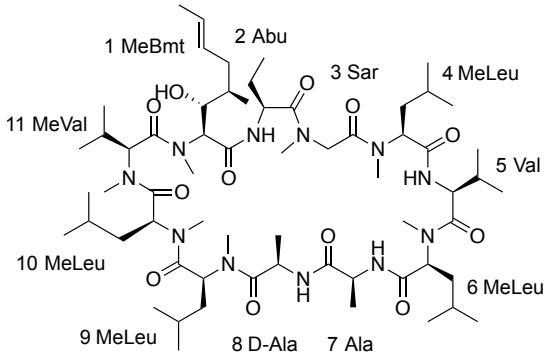

Figure (1.7) Structure of the 11-residue cyclic peptide cyclosporin A.

Another cyclic peptide from *Tolypocladium* fungi is the sulfated lipopeptide, FR190293 from *T. parasiticum*.[Kanasaki et al., 2006] The latter is the only known *Tolypocladium* species to produce conidia, asexual spores, underwater.[Barron et al., 2011] FR190293 exhibits antifungal properties against *Candida albicans*, with an IC_{50} (50% inhibitory concentration) value of 0.87 μg/mL, by inhibiting synthesis of 1, 3-β-glycan, a polysaccharide component of the cell wall. Kanasaki et al. [2006] observed high water solubility of FR190293, due to the rare sulfate group. The structure of FR190293 was elucidated by Electrospray Ionization (ESI) MS and a comprehensive NMR dataset including ^{1}H-^{1}H COSY, HSQC, HMBC and ^{13}C NMR data. However, the absolute configuration was not determined (Figure 1.8).[Kanasaki et al., 2006]

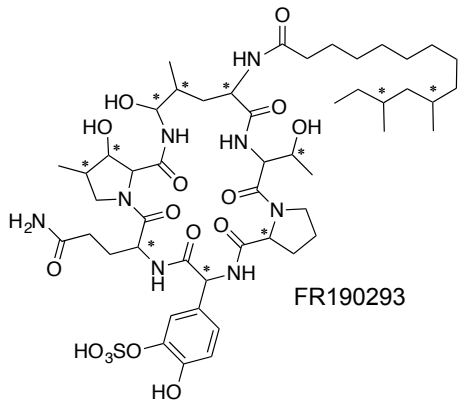

Figure (1.8) Structure of FR190293. *Stereogenic centers to be determined.

Peptaibols

Peptaibols are a class of bioactive linear peptides of fungal origin. They can range from 5-21 residues with molecular weights of 500 – 2,200 Daltons and generally contain several types of nonproteinogenic amino acids and lipoamino acids. By definition, a peptaibol includes the amino acid α-aminoisobutyric acid (Aib). Additionally, peptaibols are characterized by an acetylated *N*-terminus and have a range of C-terminal functionalities, including an acetylated amino-bonded 1,2-amino alcohol, amine, amide, free amino acid, 2,5-dioxopiperazine, or a sugar alcohol.[Degenkolb et al., 2007] One commonly found peptaibol series is the 15-amino acid family of efrapeptins. First discovered by Jackson et al. [1979] the efrapeptins contain an *N*-terminal acetylated pipecolic acid and a charged heterocycle: 2, 3, 4, 6, 7, 8-hexahydro-1-pyrrole[1,2-a]pyrimidine, on the C-terminus. Figure 1.9 shows the structure of efrapeptin D displaying the linear structure and Aib residues found among the efrapeptins. Efrapeptins exhibit insecticidal properties and have been shown to inhibit mitochondrial ATPases.[Gupta et al., 1992][Krasnoff et al.,1991] Bandani et al. [2000] conducted experiments on the insecticidal activity by exposing a

panel of insects to a mixture of efrapeptins C-G from *T. niveum*. The LD_{50}, lethal dose measured by compound weight in mg per kg of insect body weight of 50% eradicated insects, showed values ranging from 30-47 ng in larvae of *Galleria mellonella* and *Manduca sexta*.[Bandani et al., 2000] Interestingly, the specific efrapeptin analogues produced are highly dependent upon the species. For example *T. geodes* and *T. cylindrosporum* predominantly produce efrapeptins F and G *in vitro*, while *T. niveum* primarily produce efrapeptins D and E *in vitro*.[Krasnoff et al., 1992] Table 1.1 displays the efrapeptins found in *Tolypocladium*.

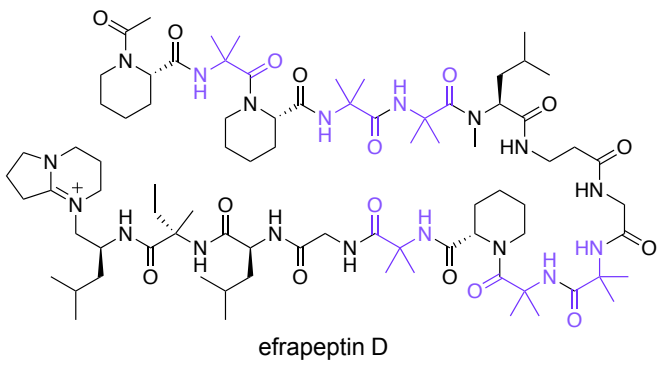

Figure (1.9) Structure of efrapeptin D. This example shows the typical linear structure of the efrapeptins and the Aib amino acid residues (in purple) required for the classification of a peptaibol.

	1	2	3	4	5	6	7	8	9	10	11	12	13	14	15	16
C	AcPip	Aib	Pip	Aib	Aib	Leu	β-Ala	Gly	Aib	Aib	Pip	Aib	Gly	Leu	Aib	X
D	AcPip	Aib	Pip	Aib	Aib	Leu	β-Ala	Gly	Aib	Aib	Pip	Aib	Gly	Leu	L-Iva	X
E	AcPip	Aib	Pip	L-Iva	Aib	Leu	β-Ala	Gly	Aib	Aib	Pip	Aib	Gly	Leu	L-Iva	X
Eα	AcPip	Aib	Pip	L-Iva	Aib	Leu	β-Ala	Gly	Aib	Aib	Pip	Aib	Ala	Leu	Aib	X
F	AcPip	Aib	Pip	Aib	Aib	Leu	β-Ala	Gly	Aib	Aib	Pip	Aib	Ala	Leu	L-Iva	X
G	AcPip	Aib	Pip	L-Iva	Aib	Leu	β-Ala	Gly	Aib	Aib	Pip	Aib	Ala	Leu	L-Iva	X
H	AcPip	Aib	Pip	L-Iva	L-Iva	Leu	β-Ala	Gly	Aib	Aib	Pip	Aib	Ala	Leu	L-Iva	X
J	AcPip	Aib	Pip	Aib	Aib	Leu	β-Ala	Gly	Aib	Aib	Pip	Aib	Ala	Leu	Aib	X

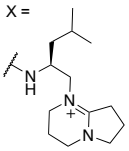

Table (1.1) Sequences of efrapeptins C-J from *Tolypocladium* species. Efrapeptins primarily contain nonproteinogenic amino acids α-aminoisobutyric acid (Aib), L-isovaline (L-Iva), β-alanine (β-Ala) and pipecolic acid (Pip). Additionally, the C-terminus comprises a positively charged 2, 3, 4, 6, 7, 8-hexahydro-1-pyrrole[1,2-a]pyrimidine (X). The figure was reproduced from [Weigelt et al., 2012].

Tsantrizos et al, [1996] have also reported the 11-residue peptaibols LP237-F5, -F7 and -F8, found in *T. geodes* LP237, as antitumor agents. The mode of action of the compounds is currently unknown, but a genotoxicity assay for human carcinoma cells provided IC_{50} values of 0.2-0.5 μg/mL.[Tsantrizos et al., 1996] These compounds are characterized by an octanoyl or decanoyl fatty acid chain on the *N*-terminus and an amino alcohol, often leucinol (Lol), on the C-terminus (figure 1.10). Interestingly LP237-F5 and -F8 also contain the unusual amino acid α-ethylnorvaline (EtNor).[Tsantrizos, Pischos, & Sauriol, 1996]

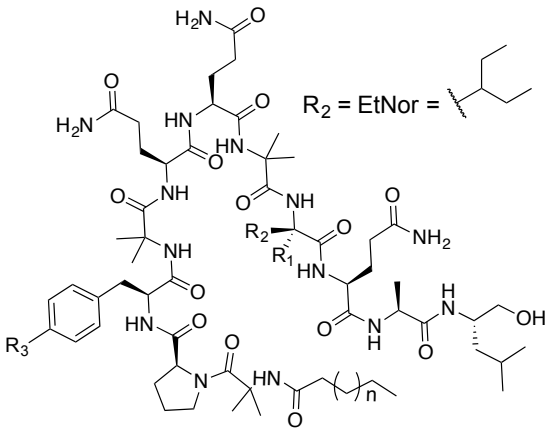

LP237-F5 R_1 = Et, R_2 = EtNor, R_3 = OH, n = 4
LP237-F8 R_1 = Et, R_2 = EtNor, R_3 = H, n = 4
LP237-F7 R_1 = R_2 = Me, R_3 = H, n = 6

Figure (1.10) Structures of the peptaibols LP237-F5, -F7, and -F8.

Tolypocladium is also known to produce the fumonisin polyketides. Gelderblom et al. [1988] first isolated fumonisins in 1988 from the species *Fusarium moniliforme MRC* 826. The agriculture industry regulates fumonisins in maize crops due to their potent toxicity when consumed by humans and animals.[Kimanya et al., 2010] The compounds are characterized by their tricarboxylic acid functionality (Figure 1.11). Specifically, fumonisins B2 and B4 have been found in *T. geodes, T. cylindrosporum* and *T. inflatum.*[Mogensen et al., 2011]

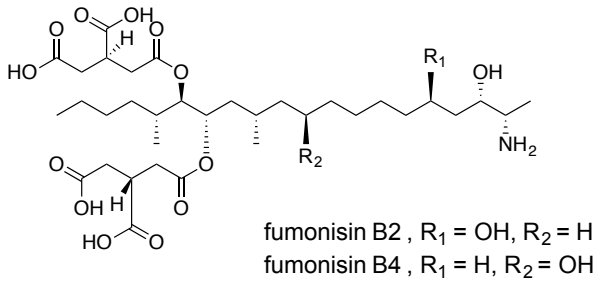

Figure (1.11) Structures of fumonisins B2 and B4.

Recently, a new tetramic acid, tolypoalbin (figure 1.12), was isolated from *T. album* and displayed adipogenic activity by inducing differentiation of pre-adipocytes to mature adipocytes.[Fukuda et al., 2015] This differentiation enabled the secretion of the peptide hormone adiponectin and reduced insulin resistance in patients with Type 2 diabetes.[Fukuda et al., 2015]

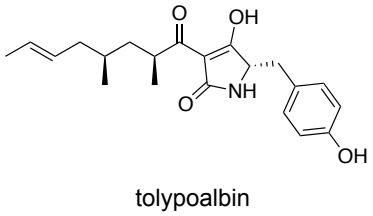

Figure (1.12) Structure of tolypoalbin

Regulation of Natural Products Expression

The hypocrealean genus *Tolypocladium* (Family Ophiocordycipitaceae) has unique switches in nutrition mode between its species.[Quandt et al., 2014] It has been shown that fungal secondary metabolites can play an important role in fungal biology and ecology. Evaluation of whole genomes in *Tolypocladium* may give insight into what secondary metabolite biosynthetic and regulatory genes may be linked to nutrient selection. This relationship can be observed through a variety of mechanisms that typically involve transcriptional regulators. For example the nutrient regulator, AreA regulates nitrogen levels and production of fumonisin B1 in *Fusarium verticillioides*.[Kim et al., 2008] Likewise, the global secondary metabolite regulator LaeA has been shown to regulate 13 of 22 secondary metabolite gene clusters in *Aspergillus*.[Bok et al., 2004] LaeA also interacts in the nucleus with developmental proteins, VelA and VelB, which upon environmental stimulus of light, determine asexual sporulation or sterigmatocystin production. [Bok et al., 2004]

Project Aims

In a collaborative effort, the Spatafora and McPhail Labs are currently investigating the *Tolypocladium* genus with the aim of identifying and comparing new and known secondary metabolites encoded in the *Tolypocladium* species genomes. The project involves whole genome sequencing, which will permit mining of secondary metabolite biosynthetic pathways. With the use of RNASeq to perform transcriptomics, expression levels of NRPS and PKS gene clusters will indicate the genes of interest involved in secondary metabolite biosynthesis for possible fungal evolutionary studies.

Identification of fungal secondary metabolite gene clusters will not only provide the functional roles of genes, but also aid in the discovery of new secondary metabolites. Chapter Two presents LC-MS profiling of the two species in different culture media, and attempts to de-replicate or assign the structures of putative new peptaibols. Chapter Three presents the metabolomic profiling of *T. inflatum* wild-type compared to a knockout mutant in which a putative secondary metabolite regulator had been deleted.

CHAPTER TWO

Metabolomic profiling of *Tolypocladium inflatum and T. geodes*

Bailey Dickey, Rheannon Arvidson, Dr. Alisha Quandt, Dr. Kathryn Bushley, Dr. Joey Spatafora, and Dr. Kerry McPhail

Introduction

Extensive phylogenomic work in the Spatafora Lab on the Order Hypocreales has revealed numerous NRPS and PKS gene clusters in *Tolypocladium inflatum*, of which the *simA* gene cluster, responsible for cyclosporin biosynthesis, has been characterized.[Bushley et al., 2013] A total of 14 NRPSs, 20 PKSs, 4 Hybrid PKS/NRPSs, 11 putative NRPS-like enzymes and 5 putative PKS-like enzymes were delineated.[Bushley et al., 2013] These gene clusters are predicted to encode both new chemistry and known natural products, some of which were not previously associated with *Tolypocladium*, such as the polyketide fumonisins, cyclic depsipeptides, and ergot alkaloids. Utilization of the gene cluster phylogenies provides a predictive tool in the search for new natural product chemistry.

The Spatafora Lab's phylogenomic analysis of the NRPS adenylation domains (A-domains) in *T. inflatum* has identified homologs of a number of functionally characterized NRPSs gene clusters and their associated metabolites. 696 NRPS A-domains from 14 hypocrealean taxa were included in the analysis, revealing homologs of NRPSs of three peptaibol synthetases (TINF05969, TINF07827, TINF07876). These putative peptaibol synthases are predicted to encode 13, 11 and 8 residues in peptaibol-like structures. Preliminary metabolomic profiling of these extracts by LC-MS/MS profiling revealed several high molecular weight compounds with peptaibol-like fragmentation patterns (Figure 2.1).

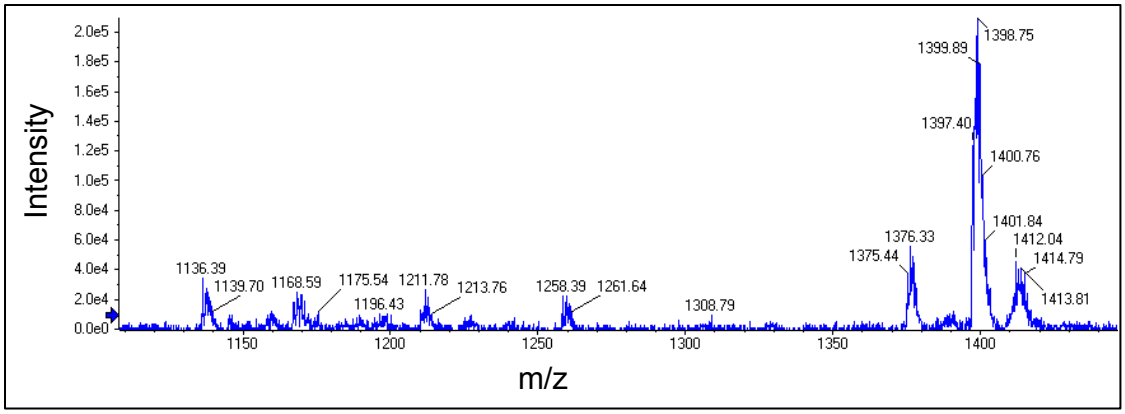

Figure (2.1) LC-MS spectrum of high molecular weight metabolites from *T. inflatum* that may be products of the putative peptaibol synthetases. RT = 38.8 min using an AbSciex 3200 QTRAP spectrometer, RP_{18} Fusion 100 x 2.0 mm HPLC column with a gradient profile of 65-100% MeOH-H_2O over 50 min followed by a 10 min hold in 100% MeOH.

Methods and Materials

Culturing. *T. inflatum W. Gams* NRRL 8044 strain was obtained from NRRL and provided by the Spatafora lab. *T. inflatum* was grown for 2.5 weeks on cornmeal agar to induce sporulation. For culturing, spore slurries obtained from agar plates were used to inoculate 100 mL of potato dextrose broth (PDB) supplemented with L-valine or synthetic medium (SM) [Chun & Agathos, 1989] cultures and incubated for six days. Culture tissues were separated from the media by filtration, lyophilized and weighed. *Tolypocladium geodes W. Gams* was grown on cellophane on potato dextrose agar (PDA). After 7 days of growth the cellophane with fungal growth was collected for extraction.

Extraction. Following lyophilization, fungal tissue was chemically extracted to yield aqueous and organic samples. The cells were soaked in MeOH-H_2O (1:1) for the aqueous extraction, and CH_2Cl_2-MeOH (2:1) for the organic extraction. In all

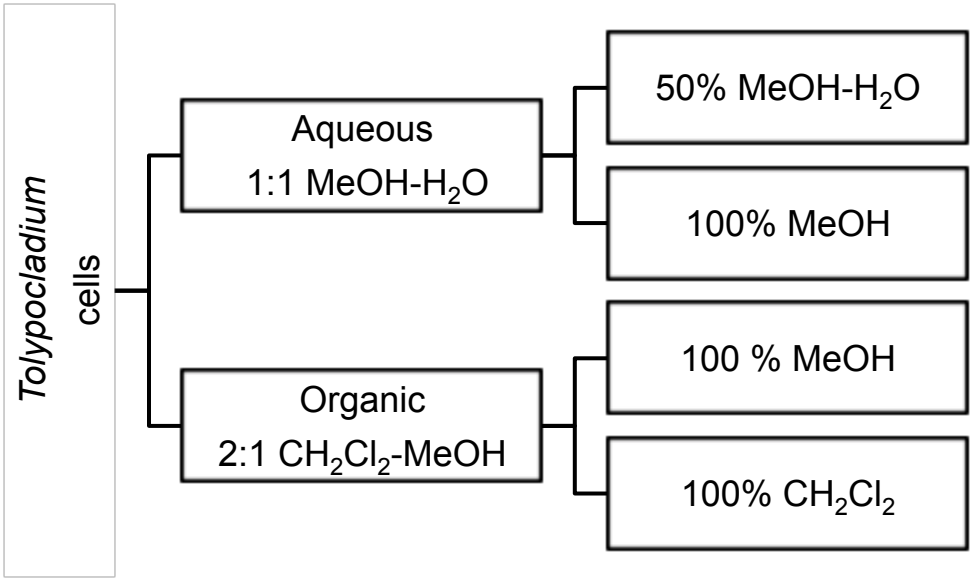

Figure (2.2) Extraction and Pre-fractionation of extracts in preparation for LCMS profiling. *Tolypocladium* samples were chemically extracted to yield an aqueous and an organic extract. Each extract was passed through a RP_{18} SPE cartridge to yield two fractions per extract. The 100% MeOH SPE fractions from the organic extracts were used for metabolomics profiling by LC-MS/MS (ES+).

instances the aqueous extraction occurred following the organic extraction. Extractions were stirred at 35 °C for 3 hours with either 50 or 150 mL volumes of the appropriate solvent mixture. The fungal cells were separated from the extraction solvent by vacuum filtration using a Büchner funnel and the extraction solvent was concentrated *in vacuo*. Individual extracts were fractionated using either a 1 g or 500 mg RP_{18} SPE cartridge. For the aqueous extracts, SPE cartridges were eluted with 50% MeOH-H_2O and 100% MeOH; for the organic extracts, SPE cartridges were eluted with 100% MeOH and 100% DCM. The resulting two fractions from each extract were concentrated in *vacuo*, weighed and resuspended as 2 mg/mL stock solutions in 4:1 MeOH-H_2O.

Sample Profiling and HPLC Peak Collection. LC-MS and LC-MS/MS (ES+) data were recorded on an AbSciex 3200 QTRAP mass spectrometer and evaluated in PeakView 2.1 software (ABSciex). HPLC analyses were conducted on a Shimadzu HPLC system equipped with two LC-20AD pumps and an SPD-M20A photodiode array detector. Stock solutions (2 mg/mL) of the SPE fractions were chemically profiled using LR-LCMS (ES+). A standard profiling method was used through the course of the study, unless stated otherwise. Samples were profiled using 10 μL injection volumes and separated using a linear gradient of 20-100% CH_3CN-H_2O/0.1% FA for 20 min with an additional hold in 100% CH_3CN/0.1% FA for 15 min. A Phenomenex Kinetex C_{18} column (2.1 x 50 mm, 100 Å, 1.7 μm, 0.7 mL/min) was used in all instances for LC-MS profiling. For batch sample sequences the column was equilibrated for 10 min in 100% MeOH between samples and 100% MeOH wash injections were performed between wild-type (WT) and knock-out (KO) sample injections. For isolation of sample components, samples were fractionated and peaks collected using RP_{18} HPLC on a Phenomenex Synergi Hydro column (4μ, 4.6 x 250 mm, 0.7 mL/min, UV detection at 210, 254, 274 and 310 nm).

Base Hydrolysis and Methylation. The sample TiWT-SM-Or (organic extract of *T. inflatum* grown in SM medium) was subjected to basic hydrolysis and methylation to potentially linearize, and thus assist in the identification of, putative cyclic depsipeptides. KOH (100 μL, 1M) was added to TiWT-SM-Or extract (0.2 mg in 2 mL H_2O) and stirred for 4 hr. The mixture was neutralized with 1M NH_4Cl and solvent removed *in vacuo*. The dried extract hydrolysate and a sample of the original extract (0.2 mg, un-hydrolyzed for comparison) were subjected to methylation by

resuspension in 300 μL of MeOH, cooling to 0 °C and drop-wise addition of $TMSCHN_2$ in diethyl ether (3 μL). The mixture was then warmed to room temperature and stirred for 4 hr. Any excess $TMSCHN_2$ was quenched with 2 μL of acetic acid. Products were labeled TiWT-SM-Or-M for methylation only and TiWT-SM-OR-BHM for basic hydrolysis + methylation. The samples were then prepared for LC-MS/MS analysis following the protocol outlined above for RP_{18} SPE.

Mild Acid Hydrolysis. Dried extract TiWT-SM-Or (4 mg) was re-suspended in 2 mL of 3N HCl with constant stirring at 100 °C. Four subsamples (500 μL) of the reaction mixture were collected at consecutive 30 min intervals, concentrated to dryness and prepared as stated above for LC-MS/MS analysis. These four mild acid hydrolysis extracts were labeled sequentially TiWT-SM-OR-MH1-4.

Results and Discussion

Putative peptaibols from *T. inflatum* cultured in PDB and SM media

Preliminary work on this project, performed by Mariko Nonogaki and Kerry McPhail, previously yielded sample Ti8044_PDB_M (355 mg, 100% MeOH SPE fraction from a 75% MeOH-H_2O extraction of *T. inflatum* grown in PDB). Given that preliminary LC-MS analysis suggested the presence of high molecular weight peptides, this sample, which had been stored at -20 °C, was re-examined using our standardized LC-MS/MS profiling method. In the MS/MS spectra, several doubly-charged mass ions with peptide-like isotope clusters, and putative molecular masses of 1323.28, 1351.60, 1365.54 1377.50 and 1391.62 Da, were observed (Figure 2.3). Because the identity of

these metabolites is unknown, the putative molecular masses deduced may represent adducts other than H^+, including Na^+. The differences of 14 Da between apparently corresponding fragment ions in the MS/MS spectra for the different parent ions is consistent with peptaibol-like structures which differ by a methyl group in either a common hydrocarbon chain or *N*-methylation of an amide bond, which is a common functionalization in fungal metabolites.[Keller et al., 2005] Interestingly, changing from PDB to SM culture medium resulted in the same higher molecular weight mass ions as in PDB-derived extract, as well as the presence of an additional analogue giving a mass peak of 1308.46 Da (Figure 2.4).

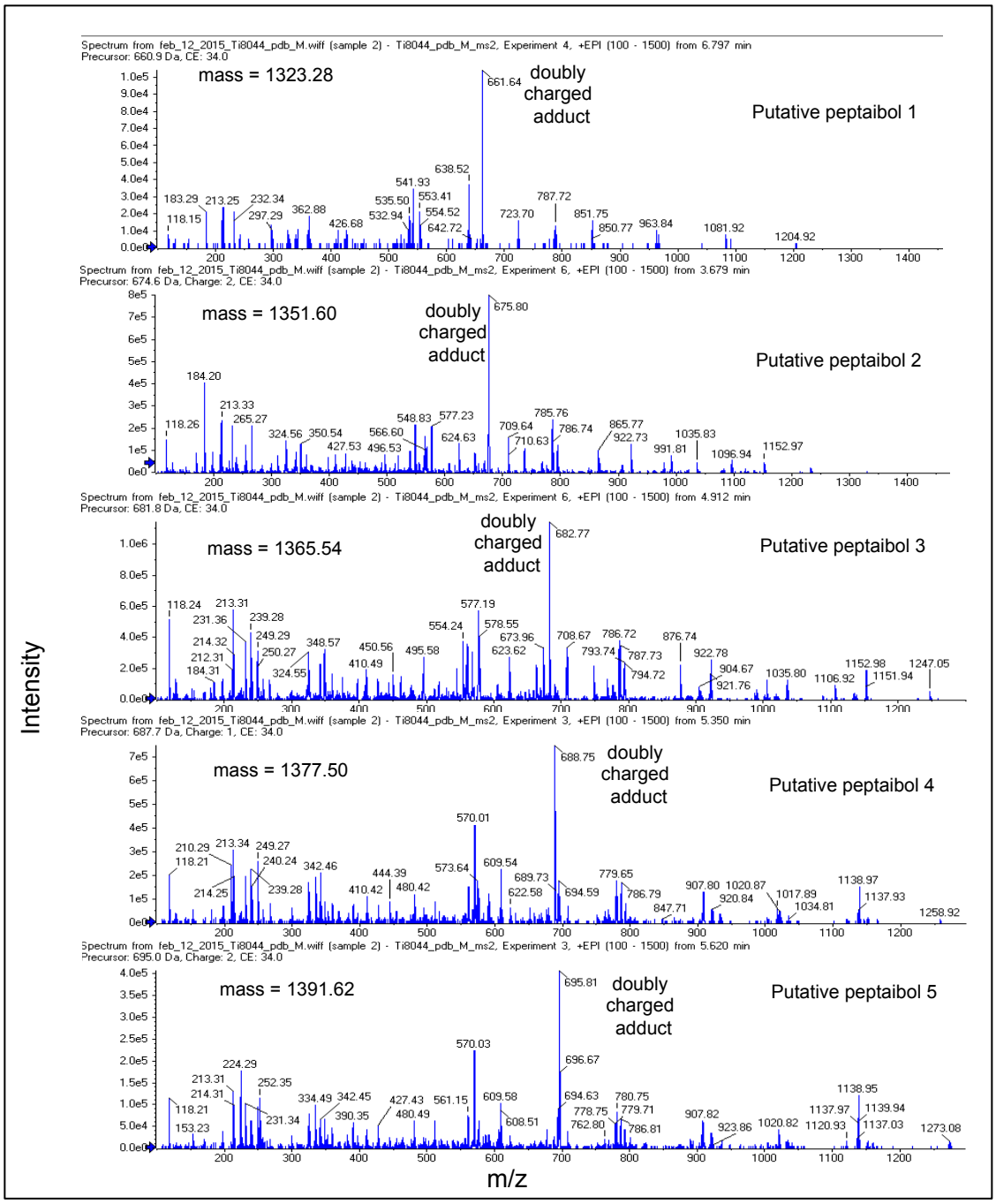

Figure (2.3) LC-MS/MS spectra for five putative peptaibols from sample TiWT-PDB-M. The differences of 14 or 28 Da between corresponding fragment ions of the five metabolites suggests that they are structural analogues.

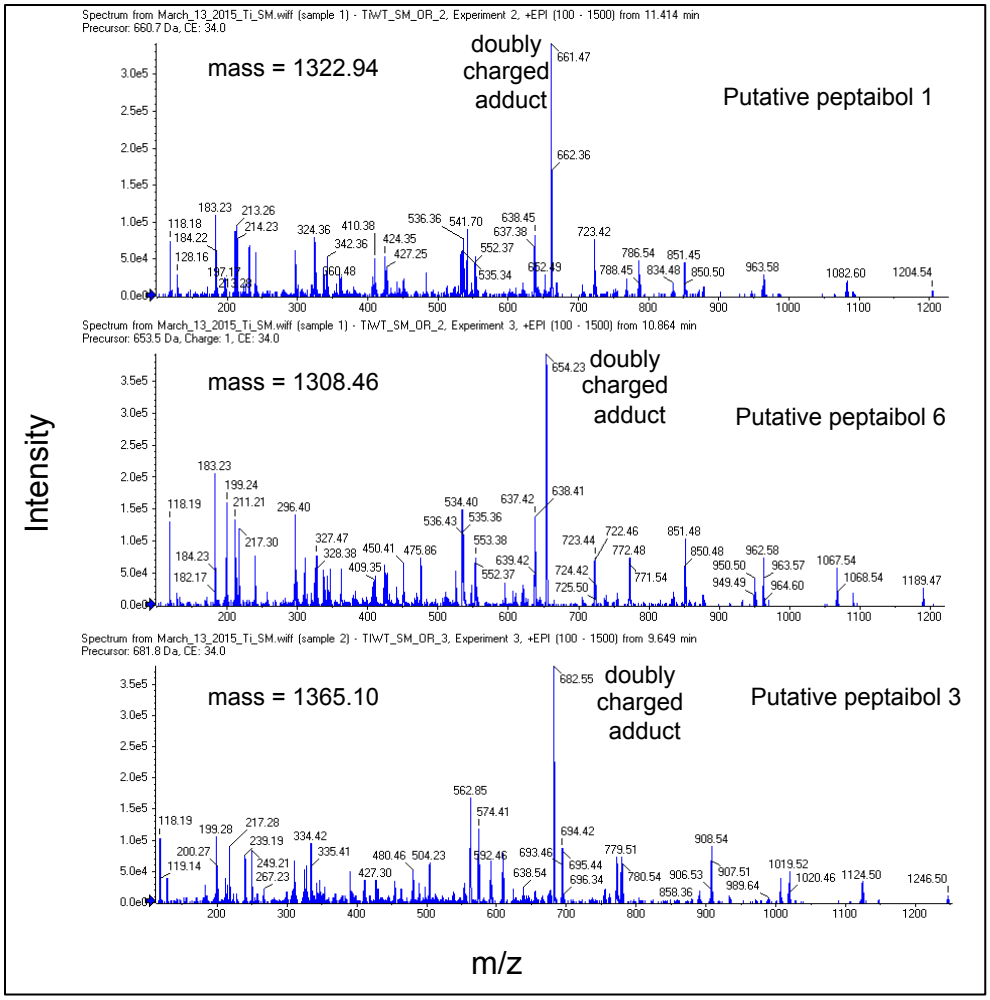

Figure (2.4) LC-MS/MS spectrum for TiWT-SM-Or-MeOH showing masses of putative peptaibols. The differences of 14 or 28 Da between corresponding fragment ions in the three spectra again suggest structurally related analogues.

The difference of 14 Da between the masses for this putative peptaibol 6 and peptaibol 1, as well as an almost identical fragment fingerprint, signals close structural analogues and implies that a change in media conditions may yield additional analogues.

It is difficult to assign specific retention times to these individual masses due to streaking on the column, possibly caused by peptide aggregation. One way to address

this challenge would be to heat up the column in order to de-aggregate any peptide complexes and thus enable more defined, sharper peaks for each peptaibol. Due to the small amounts of material used for the metabolic profiling, rigorous characterization (including NMR spectroscopy) to elucidate the structures of these putative new peptaibols has yet to be performed. However, predictions of NRPS gene clusters using the online bioinformatics tool antiSMASH only identified two NRPS/PKS clusters that were large enough to produce metabolites with these higher masses: the cyclosporin gene cluster *simA* and a larger NRPS/PKS gene cluster. Based on homology of the single adenylation domains reported from Bushley et al. [2013] and the predicted gene clusters, it is suggested that the larger NRPS gene cluster is related to these putative peptaibols.

Additional known chemistry found in *T. inflatum* and *T. geodes*

Preliminary metabolomics data has also identified known compounds associated with *T. inflatum* and *T. geodes*. Based upon the mass spectrometric data, *T. inflatum* contained cyclosporin A (Figure 2.5), as well as a number of unidentified analogues related to the cyclosporin family. CsA could be identified readily by the presence of its protonated molecule, together with a sodium adduct and a doubly charged molecular ion. The MS/MS data also showed the correct fragmentation pattern observed previously for CsA, which was found in extracts of *T. inflatum* grown in both SM and PDB media, and was also produced and identified from the extracts of *T. geodes* (Figure 2.6).

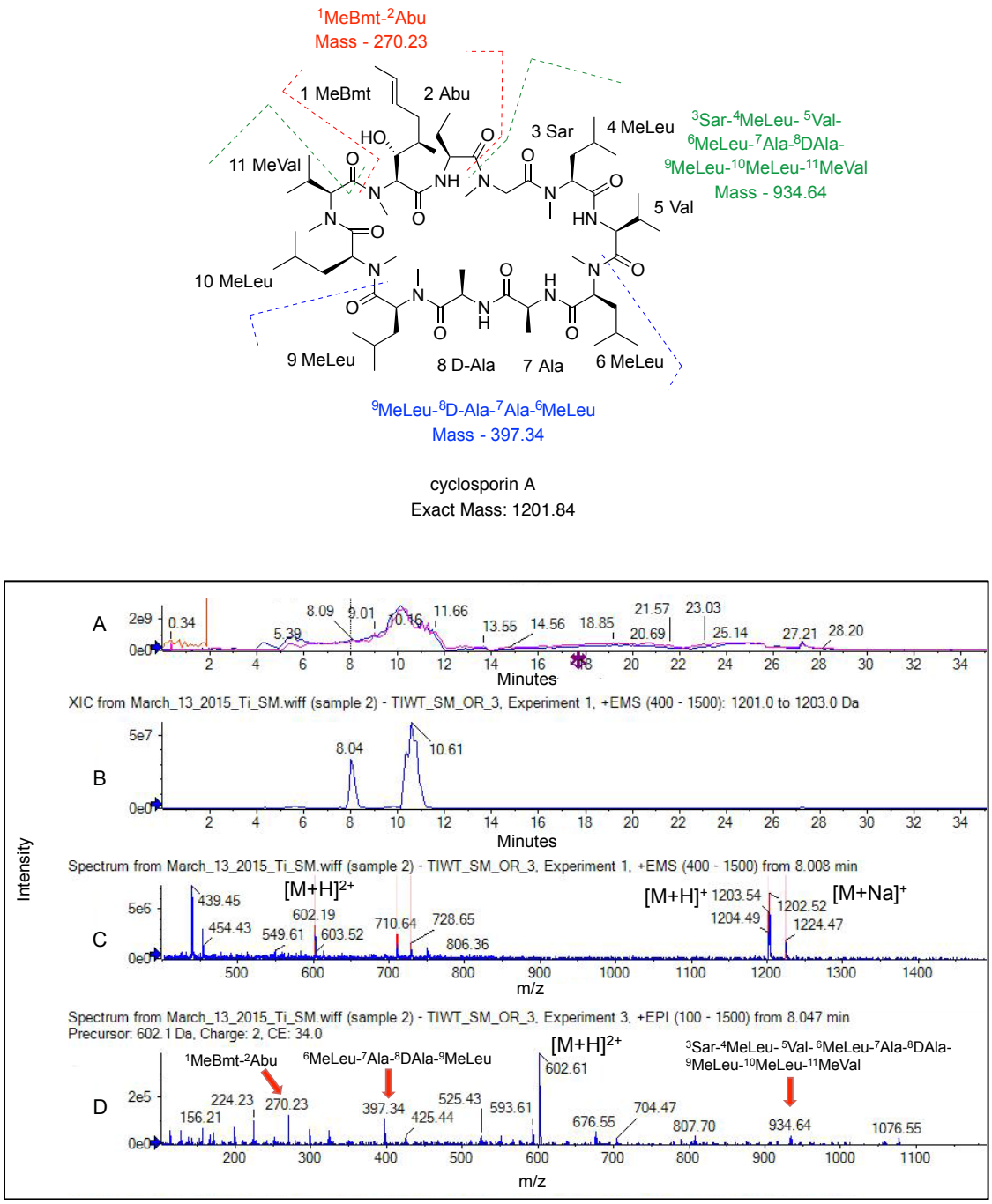

Figure (2.5) LC-MS/MS data for an extract of *T. inflatum* cultured in SM medium that contains CsA. The structure of CsA is depicted above the chromatographs. (A) Total ion count (TIC) chromatograph for *T. inflatum* extract. (B) Extracted ion count (XIC) chromatograph for molecular mass 1202, $[M+H]^+$ for CsA. (C) Mass spectrum for XIC peak at 8.0 min (CsA), with $[M+H]^+$, $[M+Na]^+$ and $[M+H]^{2+}$ labeled. (D) The MS/MS spectrum for the CsA peak. Selected characteristic fragment ions are indicated on the spectrum. The fragment ions are also depicted on the structure of CsA above. Identical results were obtained for *T. inflatum* grown in PDB medium.

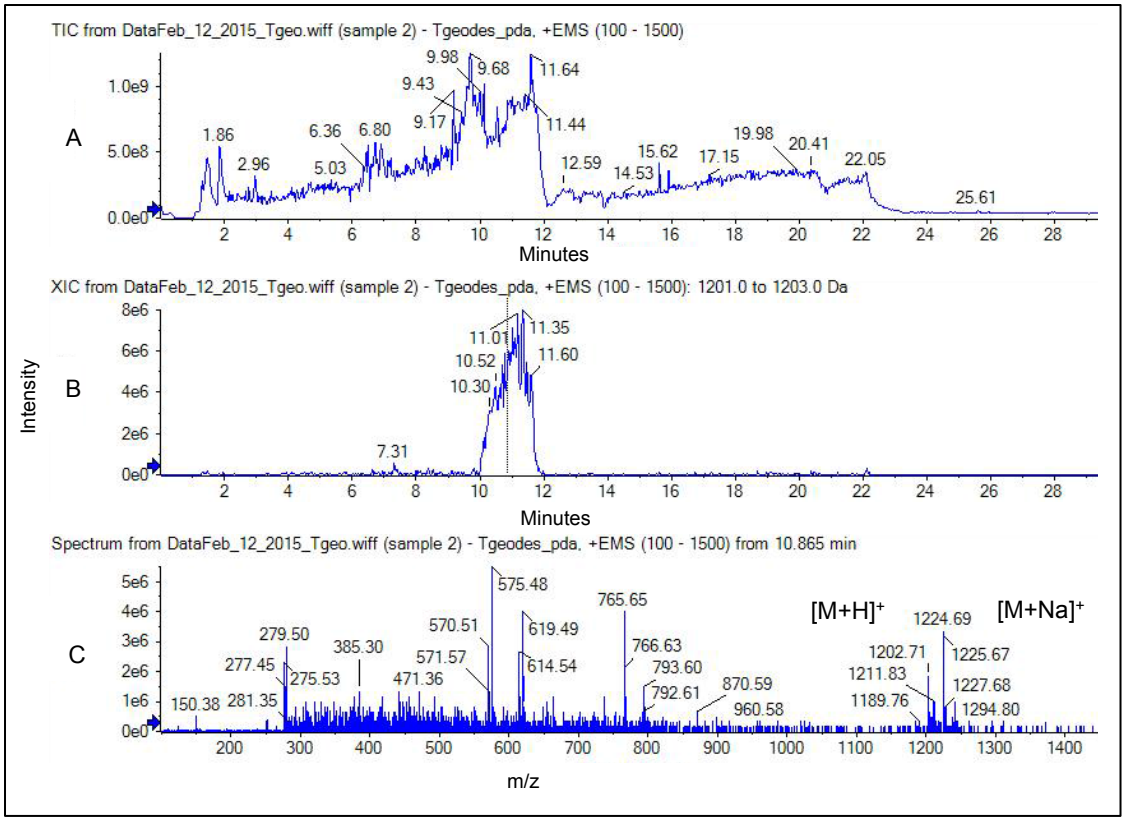

Figure (2.6) LC-MS/MS data for an extract of *T. geodes* cultured on PDA medium that contains CsA. (A) TIC chromatograph for *T. geodes* extract. (B) XIC chromatograph for molecular mass 1202, $[M+H]^+$ for CsA. (C) Mass spectrum for XIC peak at 10.9 min (CsA), showing $[M+H]^+$ and $[M+Na]^+$.

A second class of natural products identified was the fumonisins B2 and B4. These polyketides were readily identified from their unique fragmentation patterns showing a loss of one or both tricarboxylic acid (TCA) units. The presence of a large number of hydroxy groups also gave rise to the loss of H_2O units. Interestingly, it appears that there are a number of fumonisins that have not yet been reported from *T. inflatum*, but have been found in other hypocrealean fungi (Figure 2.8).[Musser et al. 1997] In addition to fumonisins B2 and B4, metabolomic profiling revealed additional MS/MS fragmentation patterns characteristic for other fumonisins. Putative structures of these are presented in Figure 2.7.

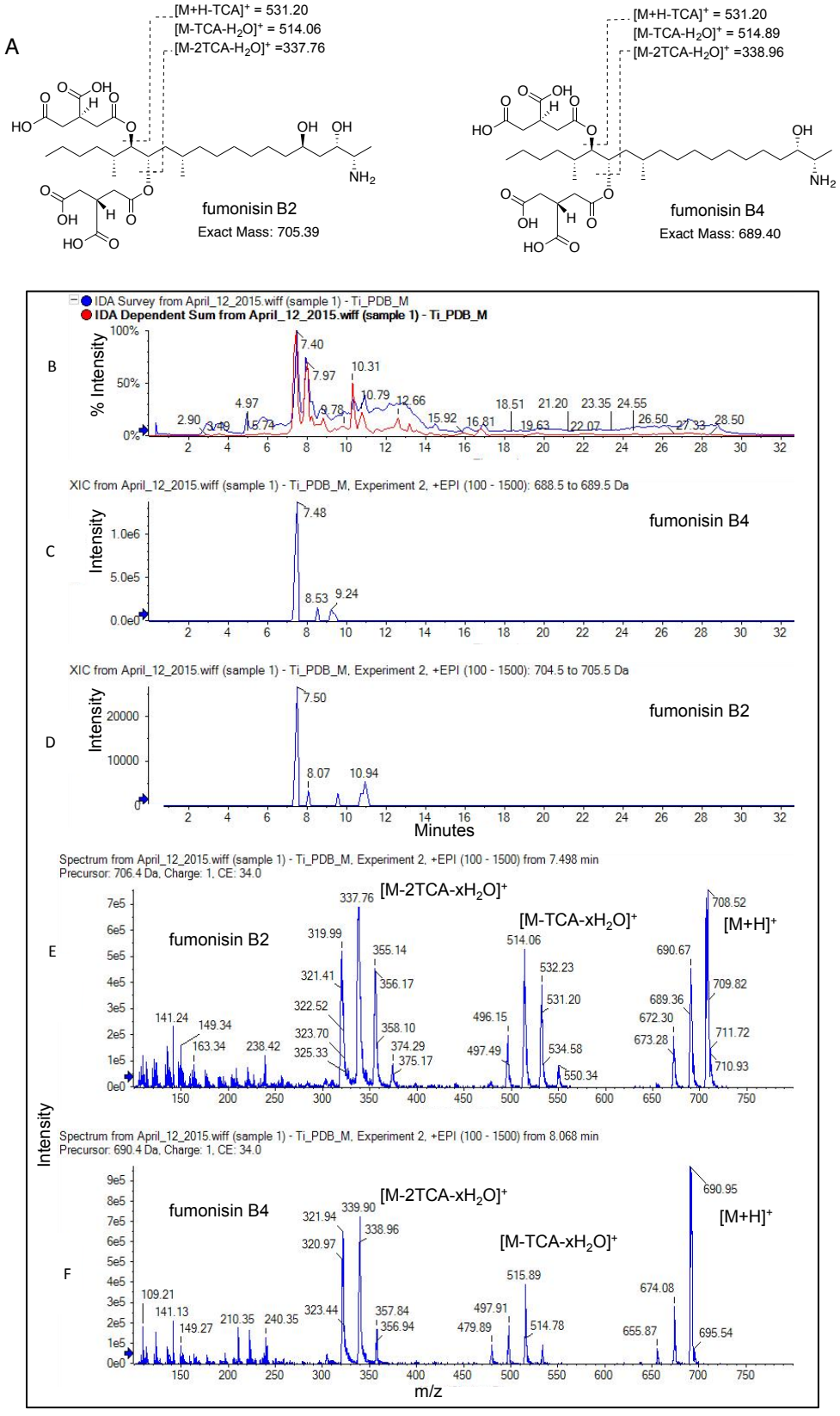

Figure (2.7) Metabolomic profiling identified known fumonisins in Ti-PDB-M. (A) Molecular structures of fumonisins B2 and B4. (B) TIC chromatograph for Ti-PDB-M.

The vertical axis represents % intensity of each peak relative to the most intense signal on the chromatograph. (C) XIC of *m/z* 689, which corresponds fumonisin B4. (D) XIC of *m/z* 705, which corresponds to fumonisin B2. (E) MS/MS spectrum for the XIC peak at 7.5 min shown in C. (F) MS/MS spectrum for the XIC peak at 8.1 min shown in D. Fragment ions are labeled in the spectra and on the structures above.

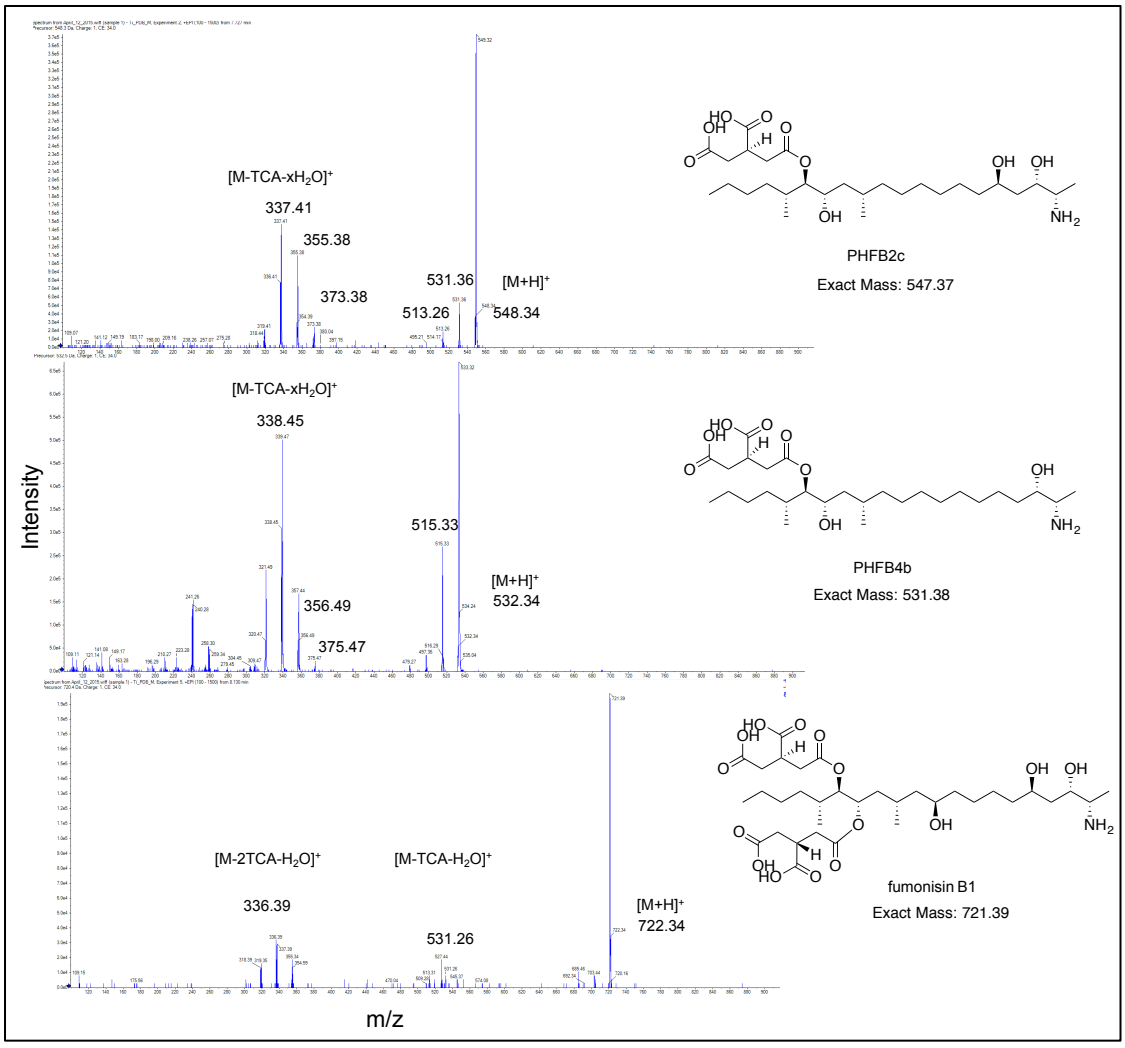

Figure (2.8) Metabolomic profiling identified fumonisins not previously reported from *T. inflatum*. The MS/MS spectrum is shown for each compound identified. In each instance the characteristic loss of TCA suggested a fumonisin analogue.

The well known family of efrapeptins were characterized from *T.geodes*. Efrapeptins F and G differ by one amino acid, with efrapeptin F having the amino acid Aib, while

efrapeptin G has L-iso-valine (Iva). This difference is evident in the MS/MS fragmentation patterns (Figure 2.9), which also delineate the loss of acetylated pipecolic acid (126 Da).

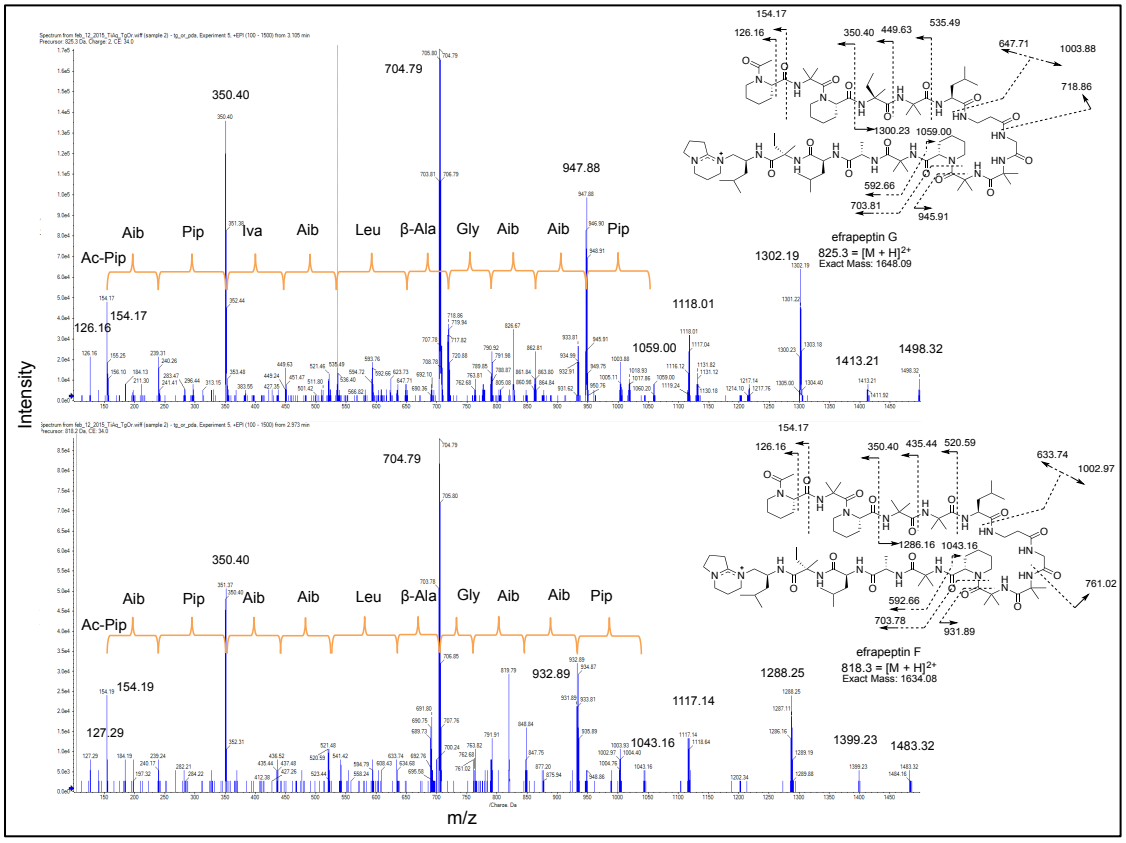

Figure (2.9) Metabolomic profiling identified efrapeptins previously reported from *T. geodes*. The MS/MS spectra for each dereplicated metabolite is shown. The sequential loss of amino acids is labeled above the mass peaks.

HPLC fractionation of putative peptaibols

The detection of peptaibols in Ti8044-PDB-M by LC-MS/MS profiling led to fractionation of this sample by HPLC, to attempt to purify these compounds in sufficient quantities to confirm their identities by HRMS and NMR spectroscopy as appropriate and necessary. A total of 15 fractions were collected by HPLC and were

assigned the nomenclature shown in Figure 2.10. In principle, the HPLC trace can be separated into three sections, those fractions that eluted at the beginning of the run (fractions B0 through B4), those that eluted at the middle of the trace (fraction C0 to C2) and those towards the end of the run (I through D).

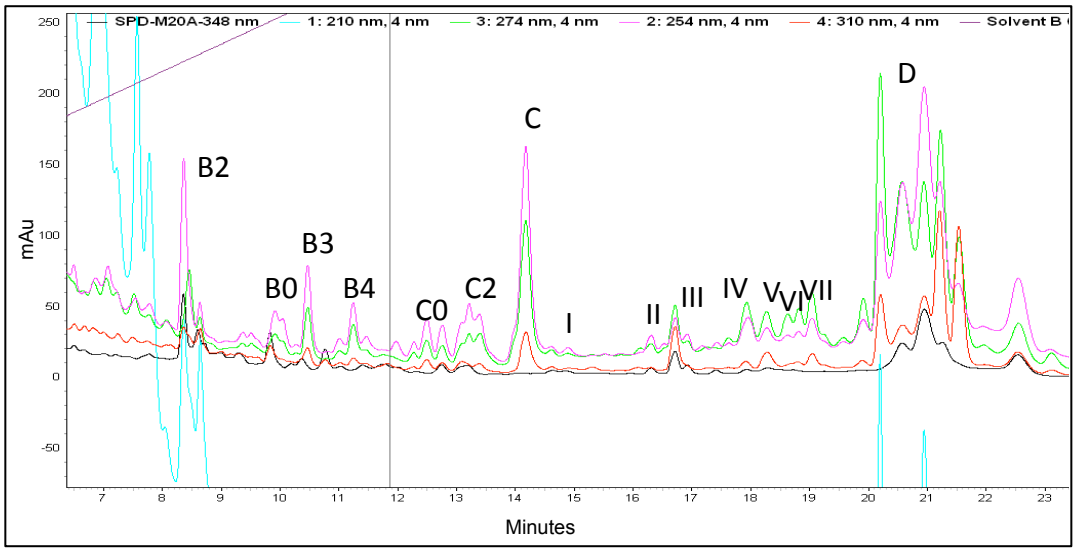

Figure (2.10) HPLC trace for Ti8044-PDB-M, which was separated into fractions B2 (8.3-8.5 min), B0 (9.8-10.0 min), B3 (10.4-10.6), B4 (11.0-11.5 min), C0 (12.4-12-9 min), C2 (13-13.7 min), C (14.0-14.2 min), I (14.6-15 min), II, III (16.8-17.0 min), IV (17.8-18.0 min), V (18.3 min), VI (18.5-18.9 min), VII (19.0-19.1 min), D (20-22 min).

The most striking peak in the chromatogram was labeled C. The increased intensity coupled with the baseline resolution led to the assumption that this may be the easiest peak to isolate and thus propose the class of compound in the neighboring fractions. Isolation and further analysis of fraction C suggested that it was CsA, since both *m/z* 1202 $[M+H]^+$ and 1224 $[M+Na]^+$ were present in the sample. To confirm this, a commercial standard of CsA was analyzed by LC-MS/MS. Ion extraction of the $[M+H]^+$ and $[M+Na]^+$ peaks showed almost identical retention times to those for

fraction C. Interestingly, in line with previous samples, CsA did not produce a sharp, well-defined peak, but instead a broad peak that eluted over a one minute time-frame was observed, suggesting peptide aggregation (Figure 2.11).

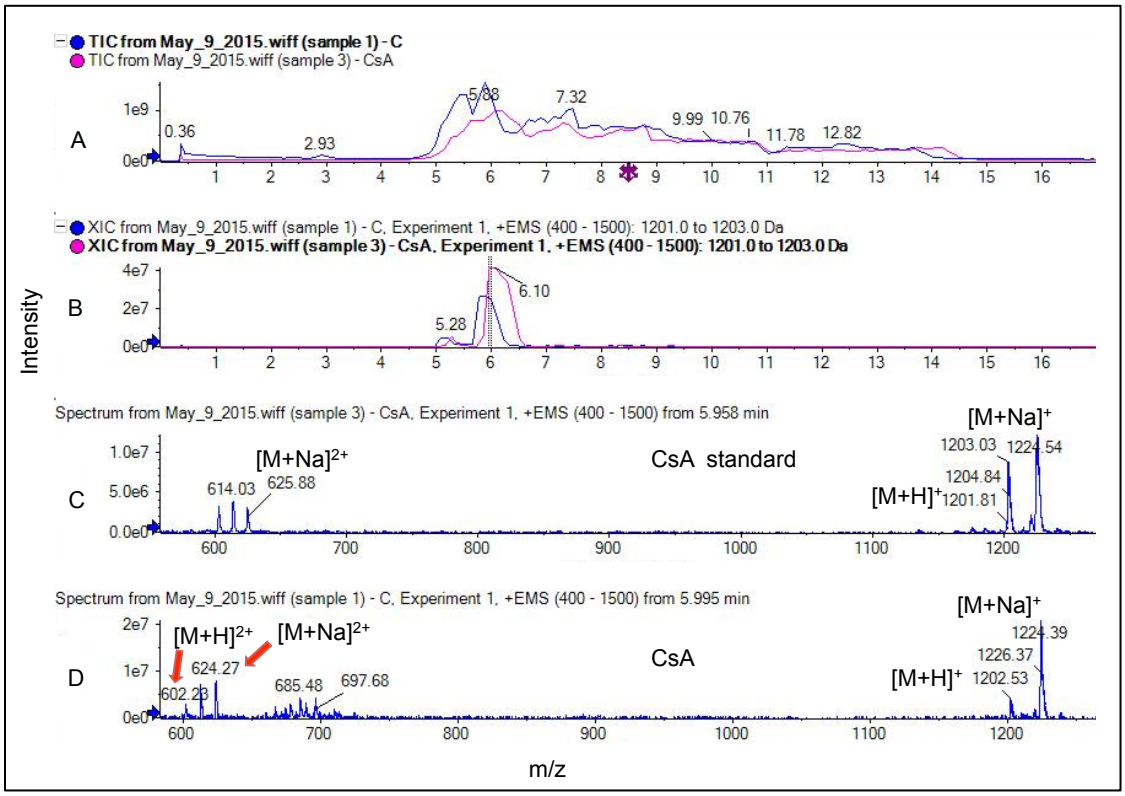

Figure (2.11) Metabolomic profiling identified CsA in fraction C from the HPLC trace of Ti8044-PDB-M and LC-MS spectrum of authentic CsA. (A) TIC of fraction C containing CsA. (B) XIC showing retention time of *m/z* 1202 for CsA in fraction C (blue) and CsA standard (pink). (C, D) Mass spectra corresponding to the XIC peaks for standard CsA and CsA in fraction C.

Further evidence to confirm the identity of CsA in fraction C was obtained from NMR spectroscopy. ^{1}H NMR of authentic CsA showed the expected *N*-methyl singlets, 11 alpha proton signals, as well as amide proton signals for the peptide scaffold (Figure 2.12). Both the chemical shifts and integrations of the peaks were in accordance with the literature. Analysis and comparison of this ^{1}H NMR spectrum to that for fraction C revealed an identical chemical shift pattern (Figure 2.13).

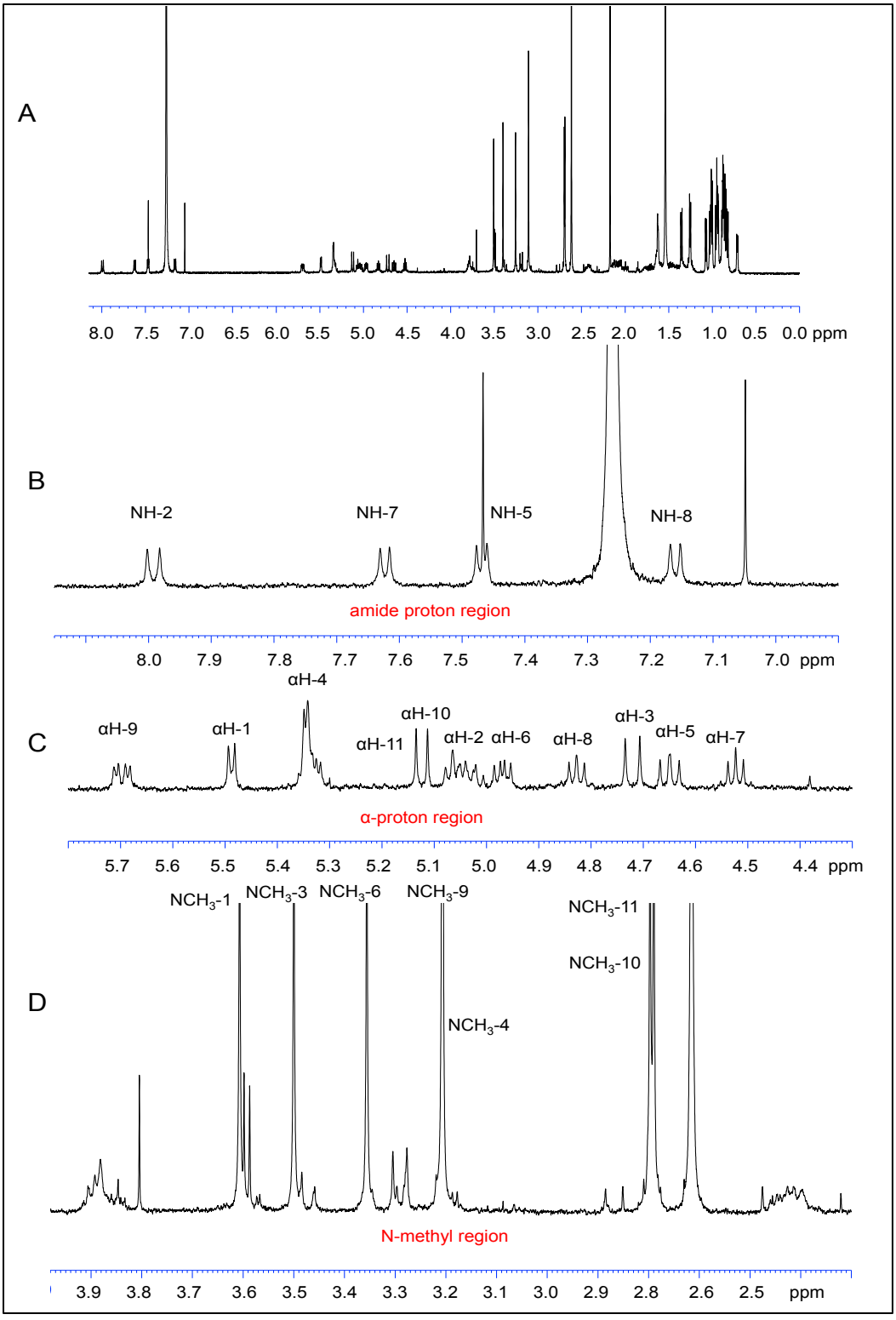

Figure (2.12) ^{1}H NMR spectrum for authentic CsA standard in $CDCl_3$ at 500 MHz. (A) Full spectrum. (B) Expansion of amide proton region. (C) Expansion of alpha proton region. (D) Expansion of *N*-methyl region.

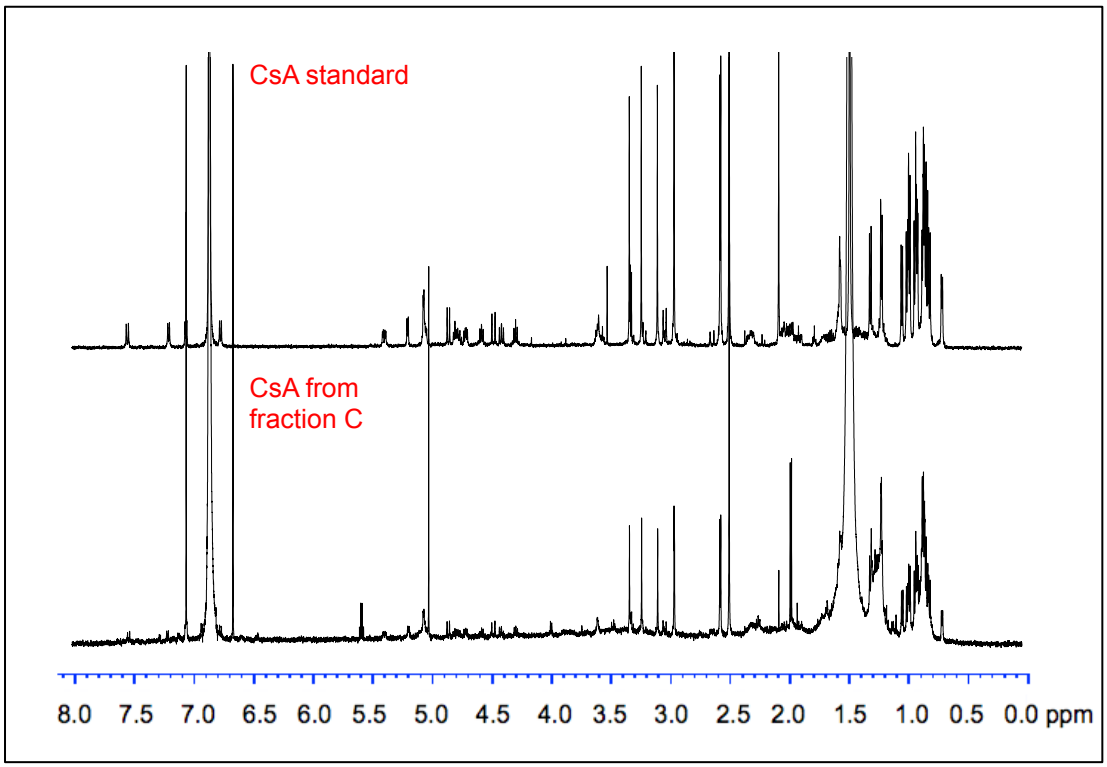

Figure (2.13) Comparison of the ^{1}H NMR spectra in $CDCl_3$ for the CsA standard and CsA isolated from fraction C. Due to the limited amount of sample from fraction C means that only the *N*-methyl and amino acid side-chain aliphatic protons are clearly visible.

LC-MS analysis of the two prefractions B4 and C0 showed the presence of putative peptaibols that were detected in the original metabolomic profiling (Figure 2.3). In fraction B4 *m/2z* 695 was present, corresponding to putative peptaibol 5 (Figure 2.14). In fraction C0 *m/2z* 681 corresponded to the peptaibol 3 (Figure 2.15). In both instances the MS/MS data showed the same characteristic fingerprints that were found in the original metabolomic profiling. Attempts to analyze either fraction by NMR spectroscopy were not successful due to the limited amount of compound isolated by HPLC. However, analysis of the LC-MS data suggested that the fractions also contained CsA due to the presence of both the $[M+H]^+$ and $[M+Na]^+$ adducts. Extracted ion chromatograms for both the putative peptaibol and CsA showed very

similar retention times and therefore indicated that the peptaibols may be aggregating with CsA, resulting in their co-elution.

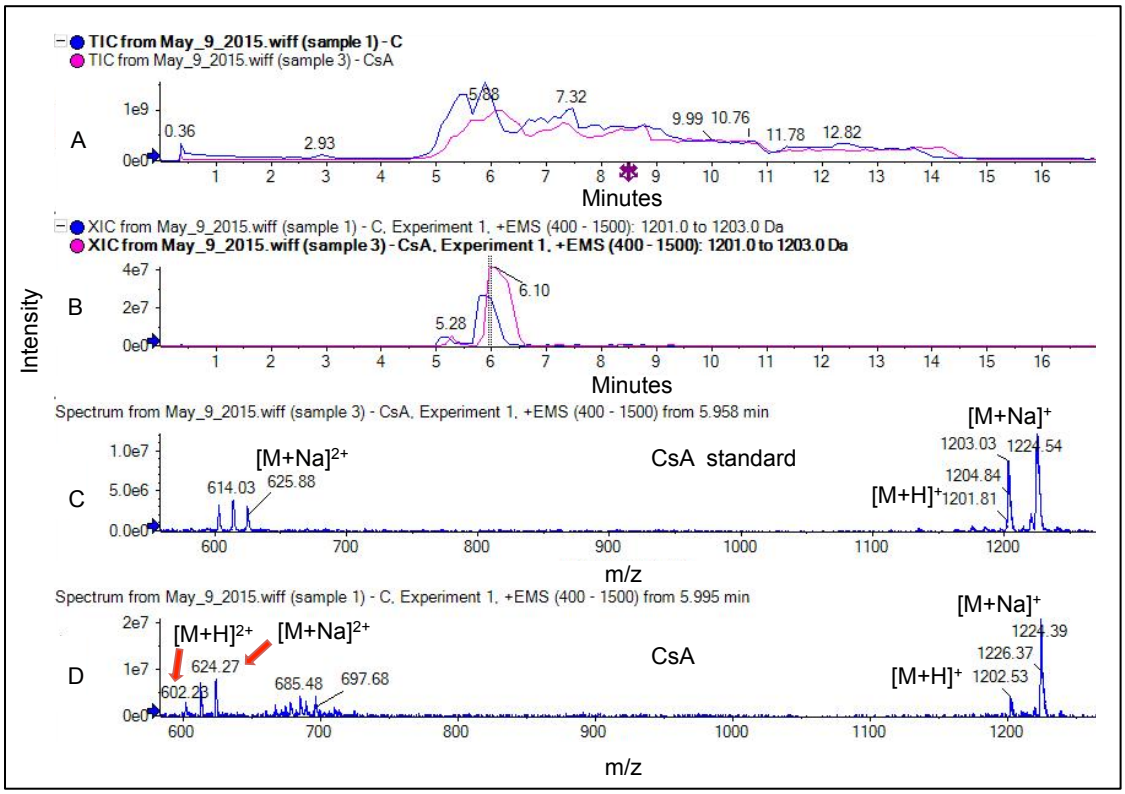

Figure (2.14) Metabolomic profiling identified putative peptaibol 5 and CsA in fraction B4 from the HPLC trace of Ti8044-PDB-M. (A) TIC chromatogram for fraction B4. (B) XIC retention times for *m/z* 1202 (CsA, blue) and 695 (putative peptaibol 5, red). (C) XIC mass spectrum showing *m/z* 1202 and 1224 for CsA. (D) XIC mass spectrum showing *m/z* 696 for putative peptaibol 5.

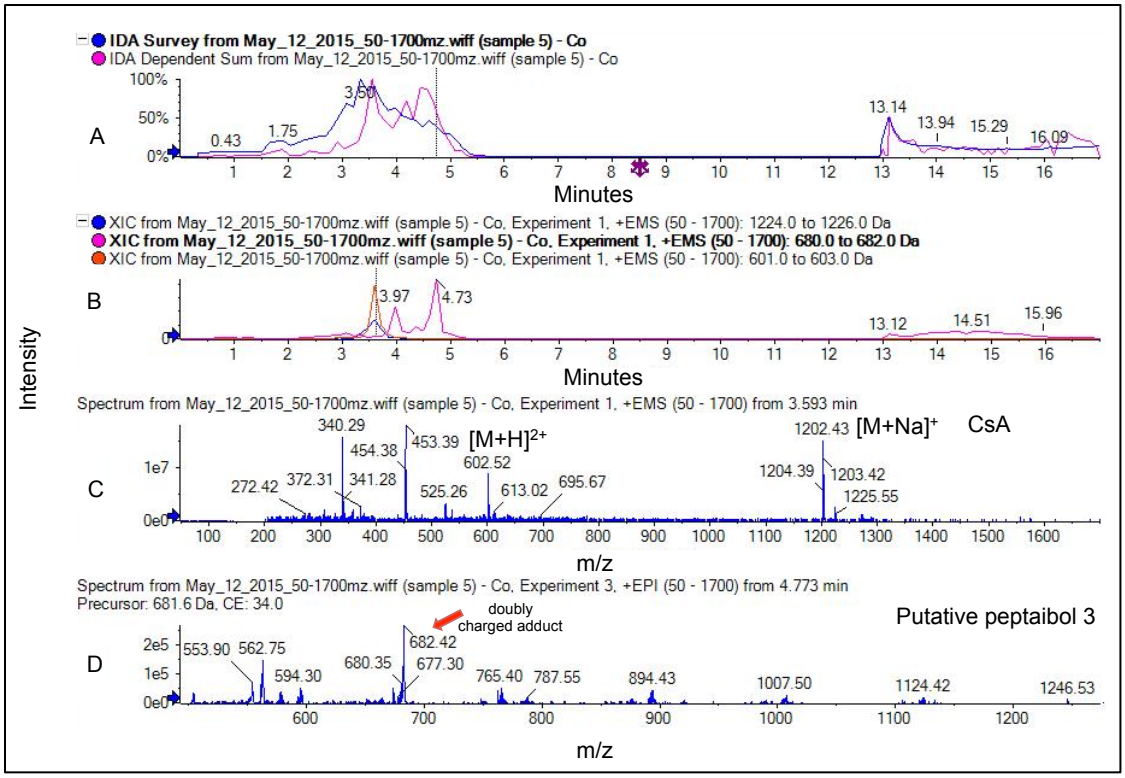

Figure (2.15) Metabolomic profiling identified putative peptaibol 3 and CsA in fraction C_0 from the HPLC trace for Ti8044-PDB-M. (A) TIC of fraction Co. (B) XIC of the masses 1224 Da and 602 Da for CsA (blue and red) and 681 Da for putative peptaibol 3 (pink). The XIC shows the retention times. (C) Mass spectrometry chromatograph of the doubly charged ion peak identified in XIC of 602 Da and sodium adduct 1224 Da, which corresponds to the mass of CsA. (D) Mass spectrometry chromatograph of peak identified in XIC. The mass 681 Da corresponds to the mass of putative peptaibol 3.

The fraction B0 was also analyzed and shown to contain fumonisin B4. Analysis of the MS data showed the presence of the molecular ion at *m/z* 705. In accordance with the original metabolomic profiling, the MS/MS data show the loss of either one or both tricarboxylic acid (TCA) units in the molecule (Figure 2.16). The characteristic sequential losses of water were also observed, in line with the previous metabolomic profiles. Interestingly, the MS data also show the presence of a fumonisin analogue not reported from *T. inflatum*. The MS/MS data show the loss of a single TCA unit, suggesting that the compound could be PHFB2c, a fumonisin previously reported from

Fusarium verticilliodes.[De Girolamo et al., 2014] Further evidence to suggest that this compound is a fumonisin lies in the very similar retention times of the two ions within the ion extraction chromatograph. However, HRMS/MS data are required, or more of the peak will need to be isolated and purified, to confirm this structural assignment.

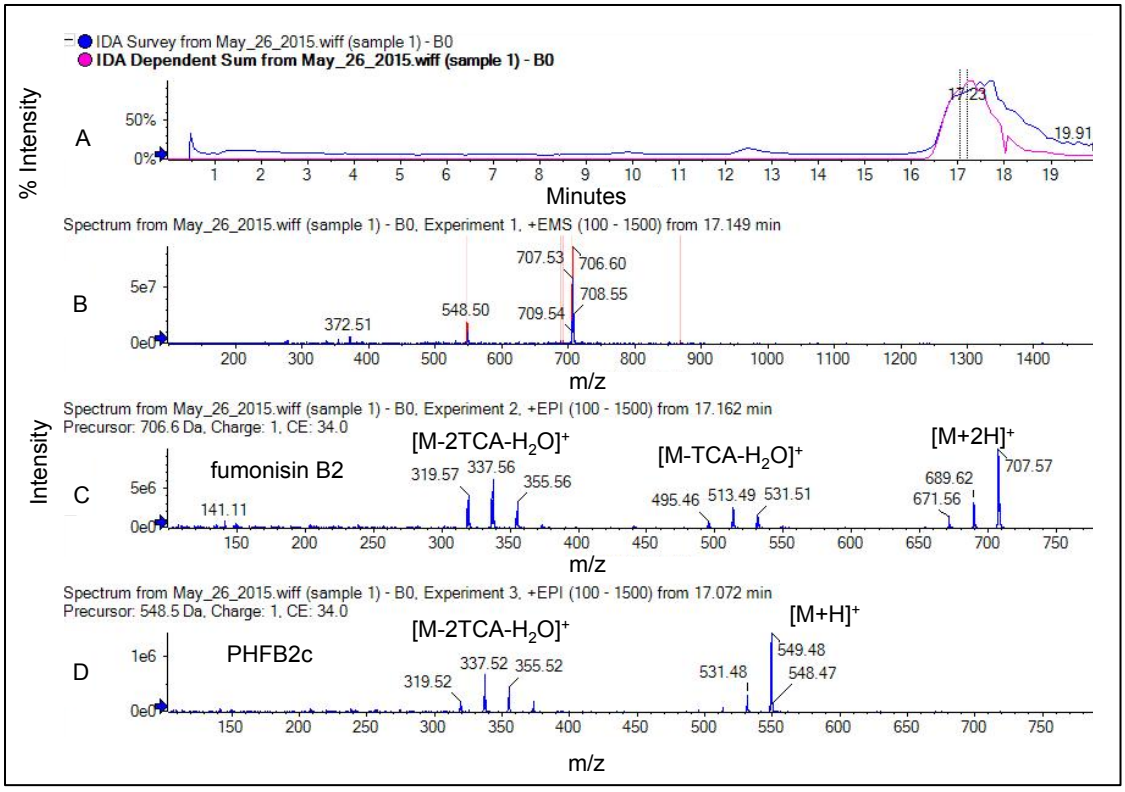

Figure (2.16) Metabolomic profiling identified fumonisin B2 and PHFB2c in fraction B0 from the HPLC trace of Ti8044-PDB-M. (A) TIC chromatogram for fraction B0. (B) Mass spectrum for time point 17.2 min in the TIC chromatogram, showing *m/z* 706.6 $[M+H]^+$ for fumonisin B2 and *m/z* 548.5 $[M+H]^+$ for suspected fumonisin PHFB2c. (C) MS/MS fragmentation of *m/z* 706.6 (fumonisin B2) in B. (D) MS/MS fragmentation of *m/z* 548.5 (putative PHFB2c) in B.

Conclusion

Metabolomic profiling of the two *Tolypocladium* species, *T. inflatum* and *T. geodes*, identified the presence of a number of secondary metabolites known to be associated with these organisms. Cyclosporin A and fumonisins B2 and B4 were identified in *T. inflatum*, and the efrapeptins F and G in *T. geodes*. In addition, a number of high molecular weight molecules designated as putative peptaibols were also to be found in the *T. inflatum* organic extract. Five putative peptaibols were noted when the organism was grown in PDB medium. Interestingly, a sixth putative peptaibol was found only in *T. inflatum* grown in SM medium, suggesting that the culture medium affects the peptaibols produced. For all six putative peptaibols, mass spectrometric data identified doubly charged ions that differed in mass by 7 Da, which would equate to a difference of 14 Da in the molecule. This mass difference suggested a relationship between the various putative peptaibols in which either elongation or contraction of the characteristic hydrocarbon chain or changes in methylation of the amide backbone had occurred.

Separation of the organic extract Ti8044-PDB-M into 15 fractions enabled identification of the major constituent as CsA. Comparative mass spectrometry and NMR spectroscopy of a known standard of CsA and fraction C confirmed that this most abundant peak in the HPLC trace of Ti8044-PDB-M contained CsA. Fractions C0 and B4 were found to contain the putative peptaibols 3 and 5, respectively. MS and MS/MS data showed the presence of doubly charged ions as well as the characteristic fingerprint of a molecule that was previously identified in the metabolomic profile. Isolation of the two putative peptaibols was problematic given that MS data indicated

the co-elution of CsA within these fractions, and insufficient material overall for NMR analysis (Figure 2.17). Finally, fraction B0 was found to contain the putative fumonisin PHFB2c, previously unknown from *T. inflatum*, as well as the known fumonisin B2. Both compounds produced the expected TCA fragmentation that is traditionally observed in the MS/MS spectra of fumonisin natural products.

Given the difficulties in separating CsA from the putative peptaibols, the following Chapter 3 will describe the attempted repression of CsA production in the hope of simplifying purification of the putative peptaibols.

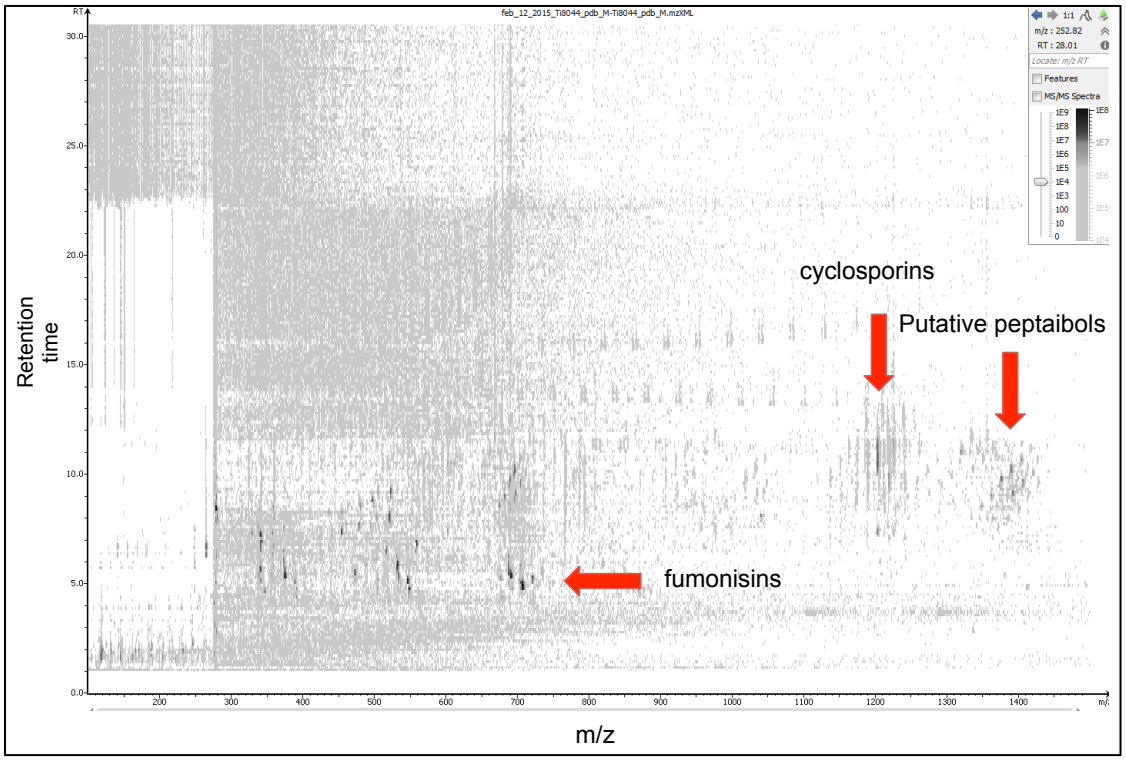

Figure (2.17) Mass spectrometric heat map of the metabolites found in extract Ti8044-PDB-M. The family of fumonisins are eluted at earlier retention times as shown. The putative peptaibols are eluted along with CsA at later retention times.

CHAPTER THREE

Loss of Cyclosporin A Production in a Genetic Knockout of a *kmt6* methyltransferase homolog in *T. inflatum*.

Bailey Dickey, Rheannon Arvidson, Mariko Nonagaki, and Igor Wierzbicki,

Dr. Alisha Quandt, Dr. Kathryn Bushley, Dr. Joey Spatafora,

Dr. Alexandra Sikora and Dr. Kerry McPhail

Introduction

Chromatin-mediated regulation in fungal secondary metabolism

One of the key ways in which secondary metabolites are regulated on a transcriptional basis is through chromatin-mediated regulation. Chromatin is a complex macromolecule comprised of DNA, RNA and proteins and is involved in packaging, regulating transcription, mitosis and preventing damage of the DNA. The principle proteins found in chromatin are histones. These positively charged proteins interact with the negatively charged DNA and cause the DNA to wrap tightly around the protein forming a complex known as a nucleosome. Typically nucleosomes occur in octamer complexes comprised of two of each of the histone proteins, H2A, H2B, H3 and H4 (Figure 3.1).

Basic transcriptional regulation can be understood by considering two main states of chromatin: heterochromatin, in which the DNA and histone interact strongly with each other forming a tightly packed complex that represses gene transcription and euchromatin, and a relaxed complex in which DNA is accessible for gene transcription. In chromatin-mediated regulation, chromatin states are controlled by post-translational modifications of histone proteins, carried out by epigenetic enzymes, which are enzymes that catalyze stable changes in gene expression without directly affecting or acting on the DNA sequence. Epigenetic enzymes covalently modify specific amino acids on the protruding tails of the histone proteins. Typically methylation, acetylation, phosphorylation, ubiquitinylation and sumoylation (small ubiquitin-like modifier) are the most common forms of histone modification, which depending upon the

functionalization of the amino acid, can either repress or activate gene transcription.[Brakhage, 2013]

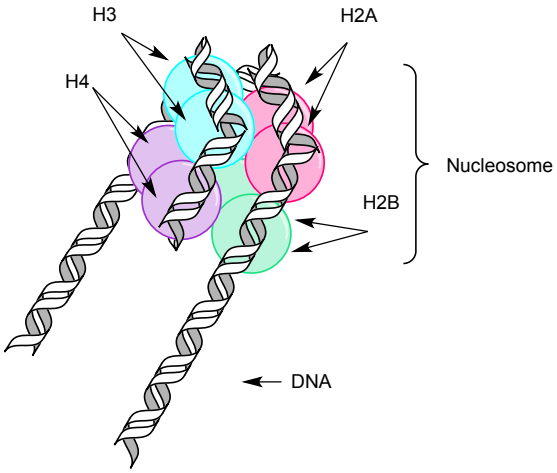

Figure (3.1) Cartoon of the structure of a nucleosome. The nucleosome is made up of two of each of the histone proteins H2A, H2B, H3 and H4 to form an octamer. The DNA wraps around the octamer to form a consolidated structure. This figure was reproduced from Georgopoulos, 2002.

There are several examples of chromatin-mediated regulation and its association with secondary metabolite gene transcription. In 2004, Bok et al. [2004] proposed the nuclear protein LaeA in *Aspergillus* spp. as a methyltransferase based on sequence similarities to arginine and histone methyltransferases. A follow-up study by Reyes-Dominguez et al. [2010] showed that deletion of *laeA* increased repressive histone 3 (H3) lysine 9 (K9) trimethylation (H3K9me3) in the sterigmatocystin gene cluster. However, the mechanism by which LaeA exerts its effect is still unknown and has not been linked directly to epigenetic control.[Bok et al., 2004] Similarly, Nützmann et al. [2011] observed a physical interaction between the fungus *Aspergillus nidulans* and the bacterium *Streptomyces rapamycinicus*, such that the bacterium induced a histone

modification that activated silent genes clusters and the biosynthesis of a polyketide, orsellinic acid. This discovery identified the H3 histone lysine 9 modifier, acetyltransferase (HAT) complex Saga/Ada in *A. nidulans* (Figure 3.2). [Nützmann et al., 2011]

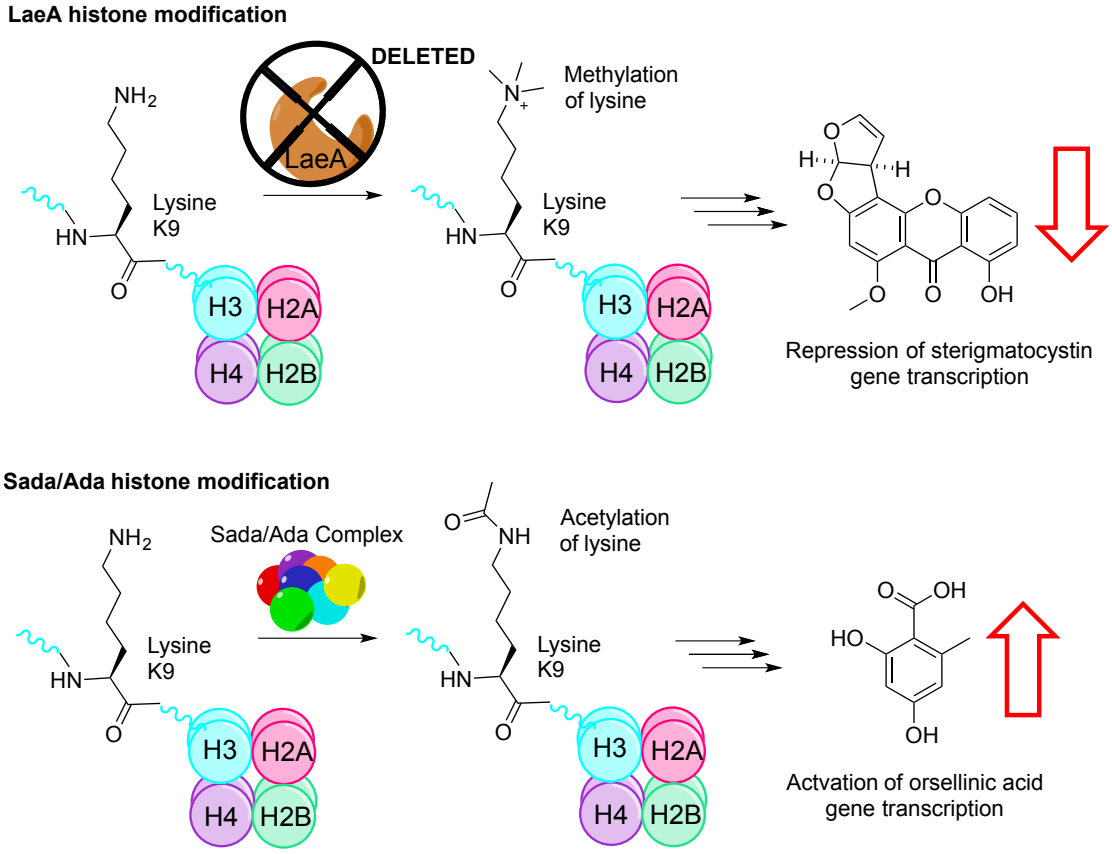

Figure (3.2) An illustration depicting two types of histone modifications on H3. Sada/Ada complex activates H3K9 by acetylation, increasing the transcription of the gene responsible for orsellinic acid. The nuclear protein LaeA represses trimethylation of H3K9me3, affecting the production of sterigmatocystin. The figure was adapted from Nützmann et al. [2011] and Bok et al. [2004].

Methyltransferase, KMT6 involved in Secondary Metabolite Expression

Histone proteins modified by methyltransferases can undergo mono-, di- and tri-methylation on lysine residues that can cause activation or repression of secondary metabolite genes (Figure 3.3). In a recent study by Connolly et al. [2013] it was found that the histone H3K27 methyltransferase, KMT6, regulates developmental growth and secondary metabolite gene clusters in *Fusarium graminearum*. Interestingly, it is a homolog of the protein *Drosophila* Enhancer of zeste, E(z) which is known to be responsible for gene silencing.[Connolly et al., 2013] It was shown that deletion of the *kmt6* gene resulted in expression of several genes for mycotoxins, pigments and other secondary metabolites. Thirty-six genes in total were derepressed in the *kmt6* knockout, including *carO* and *carX* from the carotenoid cluster and nine genes from the fusarin C cluster (*fus1*, *fus2*, *fus3*, *fus5*, *fus6*, *fus7*, *fus8*). [Connolly et al., 2013]

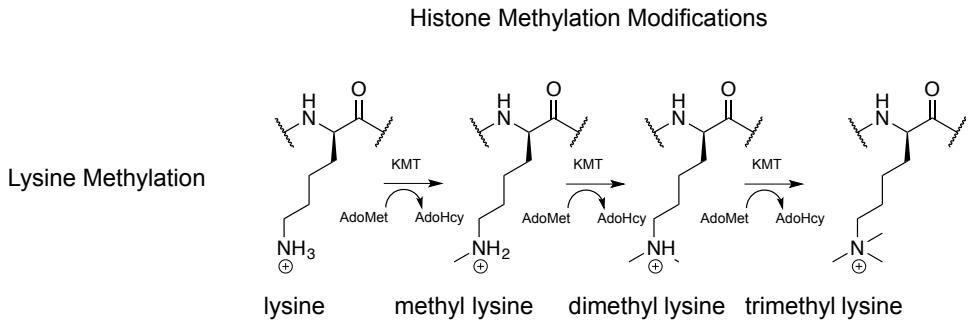

Figure (3.3) Histone modifications by methylation of lysine residues. Lysine residues can be mono-,di-, and tri-methylated by lysine methyltransferases (KMT) which catalyze the addition of a methyl group from the donor S-adenosylmethionine (SAM). The figure was adapted from [Shilatifard, 2006].

Phylogenetic analysis [Spatafora pers. comm.] revealed a homolog of the *kmt6* gene in *T. inflatum*. Given the literature precedent for such an enzyme to regulate secondary

metabolite production, it was hypothesized that a similar observation may be observed in *T. inflatum*. Therefore, a knockout mutant of *T. inflatum* was produced, which contained a deletion of the *kmt6* gene homolog. Extracts of this strain, referred to from now on as Ti-KO, were examined via LC-MS/MS for possible expression of silenced secondary metabolite gene clusters and differing metabolomic profiles to the wild type *T. inflatum*.

Methods and Materials

Culture conditions for time course and alternate media studies

Fungal strain *T. inflatum* NRRL 8044 in the Spatafora lab was obtained from NRRL (wild-type) and was used to produce the *T. inflatum* mutant with deleted *kmt6* homolog (*Δkmt6* (knockout) strain). In the Spatafora lab, both strains were grown for 2.5 weeks on cornmeal agar to induce sporulation. For culturing, spore slurries obtained from agar plates were used to inoculate 100 mL potato dextrose broth (PDB) or synthetic medium (SM) cultures.[Chun et al., 1989] SM medium was purchased from VWR and was supplemented with L-valine for all culturing. Six g/L of L-valine was added to the SM medium for all experiments examining the effects of different precursor amino acids on CsA production, except where L-valine concentration itself was the variable (0-16 g/L). For the time course study, cultures were inoculated in PDB for two, six and ten days in triplicate. For the SM media study, cultures were inoculated in SM broth in duplicate.

Labeling of fungal samples

The Spatafora lab provided all fungal culture samples for metabolomics profiling. Tables 3.1 and 3.2 list the samples with the labeling scheme used throughout the

project. In all instances, the genus *Tolypocladium* is designated by "T" and the species name by a lower case letter ("i"), followed by the nomenclature KO (*Δkmt6*, knockout) or WT (*T. inflatum* NRRL 8044, wild-type) to denote whether the *kmt6* gene has been knocked out. Following this, listed sequentially is the time course day (when harvested) or media type, replicate number, extraction method (Or = organic extract or Aq = aqueous extract) and SPE fraction (50% MeOH, 100% MeOH or DCM, dichloromethane). Aqueous and organic extracts from *T. inflatum* grown in PDB were used for the time course study and for *Neisseria gonorrhoeae* antibacterial assays. The 100% MeOH SPE fractions from the organic extracts of *T. inflatum* grown in PDB and SM were subjected to comparative LC-MS/MS-based metabolomics profiling.

Time Course	Aq. Extract Fraction	Aq. Extract Fraction	Or. Extract Fraction	Or. Extract Fraction
Day 2	TiWT-D2-X-Aq-50% MeOH	TiWT-D2-X-Aq-MeOH	TiWT-D2-X-Or-MeOH	TiWT-D2-X-Or-DCM
	TiKO-D2-X-Aq-50% MeOH	TiKO-D2-X-Aq-MeOH	TiKO-D2-X-Or-MeOH	TiKO-D2-X -Or-DCM
Day 6	TiWT-D6-X-Aq-50% MeOH	TiWT-D6-X-Aq-MeOH	TiWT-D6-X-Or-MeOH	TiWT-D6-X-Or-DCM
	TiKO-D6-X-Aq-50% MeOH	TiKO-D6-X-Aq-MeOH	TiKO-D6-X-Or-MeOH	TiKO-D6-X-Or-DCM
Day 10	TiWT-D10-X-Aq-50% MeOH	TiWT-D10-X-Aq-MeOH	TiWT-D10-X-Or-MeOH	TiWT-D10-X-Or-DCM
	TiKO-D10-X-Aq-50% MeOH	TiKO-D10-X-Aq-MeOH	TiWT-D10-X-Or-MeOH	TiKO-D10-X-Or-DCM

Table (3.1) RP_{18} SPE fractions from aqueous and organic extracts of *T. inflatum* WT/KO grown in PDB in triplicate, and harvested on days 2, 6, and 10. X denotes the replicate number from each day (D2: X = 1, 2, 3 D6: X = 4, 5, 6 D10: X = 7, 8, 9).

SM study of biological replicates	Or. Extract 100% MeOH	Or. Extract DCM
1	TiWT-SM-Or-1	TiWT-SM-DCM-1
	TiKO-SM-Or-1	TiKO-SM-DCM-1
2	TiWT-SM-Or-2	TiWT-SM-DCM-2
	TiKO-SM-Or-2	TiKO-SM-DCM-2

Table (3.2) RP_{18} SPE fractions from organic extracts of WT/KO *T. inflatum* grown in SM. Each biological replicate yielded two fractions: 100% MeOH and DCM (CH_2Cl_2).

Reversed-phase extraction. Following harvesting, all fungal cells were lyophilized to determine whether any significant differences in physical mass were observed between the wild-type and *Δkmt6* cultures. For the aqueous extraction, cells were treated with MeOH-H_2O (1:1), whilst for the organic extraction cells were extracted with CH_2Cl_2-MeOH (2:1). In all instances the organic extraction was performed after the aqueous extraction. Extractions were stirred at 35 °C for 3 hours in either 50 or 150 mL volumes of the appropriate solvent mixture, depending upon whether the mass was higher than 100 mg then, 150 mL volumes was used. Extracts were separated from the cell mass by vacuum filtration using a Büchner funnel and concentrated to dryness *in vacuo*. Percent yields were calculated by averaging the extract masses obtained for the three culture replicates in each case. Individual extracts were fractionated using either a 1 g or 500 mg RP_{18} SPE cartridge. For the aqueous extracts, SPE cartridges were eluted with 50% MeOH-H_2O and 100% MeOH; for the organic extracts, SPE cartridges were eluted with 100% MeOH and 100% DCM. The resulting two fractions from each extract were concentrated in *vacuo*, weighed and resuspended as 2 mg/mL stock solutions in 4:1 MeOH-H_2O.

Sample Profiling and HPLC Peak Collection. LC-MS and LC-MS/MS (ES+) data were recorded on an AbSciex 3200 QTRAP mass spectrometer and evaluated in

PeakView 2.1 software (ABSciex). HPLC analyses were conducted on a Shimadzu HPLC system equipped with two LC-20AD pumps and an SPD-M20A photodiode array detector. Stock solutions (2 mg/mL) of the SPE fractions were chemically profiled using LR-LCMS (ES+). A standard profiling method was used through the course of the study, unless stated otherwise. Samples were profiled using 10 μL injection volumes and separated using a linear gradient of 20-100% CH_3CN-H_2O/0.1% FA for 20 min with an additional hold in 100% CH_3CN/0.1% FA for 15 min, bringing the total run time to 35 min. All profiling was done using a Phenomenex Kinetex C_{18} column (2.1 x 50 mm, 100 Å, 1.7 μm, 0.7 mL/min). For batch sample sequences the column was equilibrated for 10 min in 100% MeOH between samples and 100% MeOH wash injections were performed between WT and KO sample injections.

Antibacterial Assay Methods. *Neisseria gonorrhoeae* (GC) isolate MS11 was propagated on GCB agar solid medium (Difco) and in gonococcal base liquid (GCBL) medium supplemented with Kellogg's supplements I (1:100) and II (1:1,000) [Kellogg et al., 1963][Spence et al., 2008]. Bacteria were streaked on a solid media plate from the freezer stocks and incubated for 18-20 h in the presence of 5% CO_2 at 37 °C. Non-piliated colonies were passaged onto fresh plates and incubated for 18 h at 37 °C with 5% CO_2. GC cells were suspended to an optical density (OD_{600}) of 0.1 in liquid media pre-warmed to 37 °C. Bacterial suspensions (100 μL) were added to a 96-well polystyrene microtiter plate (Greiner) containing 0.5 and 5 μg of fungal extracts or 1% DMSO (vehicle control) and incubated at 37 °C with aeration (150 rpm) for 9 h. OD_{600} measurements were taken at selected time points (0 h, 3 h, 6 h and 9 h).

Organic Extraction Methods. Because the aqueous extraction of *T. inflatum* grown in PDB did not recapitulate the metabolomic profile observed for previous samples (processed by Mariko Nonagaki), cell tissue was subjected to organic extraction. After washing with 150 mL of LC-MS grade water to remove excess media salts, the cells were lyophilized and then stirred in CH_2Cl_2-MeOH (2:1, 150 mL) at 35 °C for 2 h. The resulting organic extracts were then passed through a 1 gram normal-phase (NP) SPE cartridge which had been primed and equilibrated with 30 mL of 100% hexanes. Each lyophilized extract was loaded on to an SPE cartridge and eluted with 15 mL each of 100% hexanes (A), 4:1 hexanes-ethyl acetate (B), 3:2 hex-EtOAc (C), 2:1 hex-EtOAc (D), 1:4 hex-EtOAc (E), 100% EtOAc (F), 1:1 MeOH-EtOAc (G) and 100% MeOH (H), Figure 3.3. The resulting fractions E-H were concentrated to dryness and prepared for LC-MS/MS analysis as 2 mg/mL solutions in MeOH.

Normal Phase SPE Fractions from the Organic Extract for *T. inflatum* WT	NPSPE Elution Solvent
Ti-PDB-Or-A	100% hexanes
Ti-PDB-Or-B	4:1 hexanes-EtOAc
Ti-PDB-Or-C	3:2 hexanes-EtOAc
Ti-PDB-Or-D	2:1 hexanes-EtOAc
Ti-PDB-Or-E	1:4 hexanes-EtOAc
Ti-PDB-Or-F	100% EtOAc
Ti-PDB-Or-G	1:1 EtOAc-MeOH
Ti-PDB-Or-H	100% MeOH

Table (3.3) NP SPE fractions obtained from the organic extract of *T. inflatum* WT grown in PDB

Results and Discussion

Time course metabolomics profiling of *kmt6* homolog knock-out mutant versus wild-type *T. inflatum* grown in PDB medium

A homolog of the *Fusarium kmt6* methyltransferase gene was identified in *T. inflatum* as a potential key regulator of secondary metabolism in the Spatafora Lab. This gene was deleted to create a knock-out mutant, with the aim of identifying new secondary metabolites resulting from upregulated biosynthetic genes. Previous LC-MS analyses (in the McPhail Lab) of the organic extract from *T. inflatum* grown in PDB showed more diverse secondary metabolite production than from *T. inflatum* grown in other selected media. Therefore, PDB medium was chosen initially to investigate any change in secondary metabolite production in the Δ*kmt6* (homolog) knockout strain of *T. inflatum*. Cultures were grown in triplicate for two, six and ten days before harvesting to measure relative abundance and diversity of the secondary metabolites produced.

The *kmt6* knockout in *F. graminearum* by [Connolly et al., 2013] resulted in expression of an additional ~14% of the genome. This significant increase in the production of metabolites suggested that a mass difference between the WT and KO extracts could likely be detected. Therefore, in our study using *T. inflatum*, we compared extract yields in the hope of detecting mass differences that might be consistent with an increased expression of secondary metabolites. From our data, however, the total yields (Table 3.4) and the LC-MS data of extract from WT versus KO *T. inflatum* was essentially the same. The similarities between the WT and KO are shown in Figure 3.4A displaying similar TIC traces and Figure 3.4B displaying a

heatmap of similar metabolite masses. This implies no dramatic changes in secondary metabolite gene expression and production. Of course, there are many factors that could account for no direct link between extract mass and upregulation of secondary metabolite biosynthetic genes, including optimal media selection or expression of genes that may de-repress other genes, but the LC-MS data provides further evidence that the KO resembles the WT (Figure 3.4). Further investigations are needed to identify possible gene upregulation by performing transcriptomics to obtain RNASeq data.

Time Course	*T. inflatum* in PDB	Aq. Extract % Yield	Or. Extract % Yield	Total % Yield
Day 2	TiWT	7.43	0.72	8.15
	TiKO	11.38	0.57	11.96
Day 6	TiWT	16.70	2.41	19.11
	TiKO	17.44	1.31	18.7
Day 10	TiWT	7.40	0.68	8.07
	TiKO	9.56	0.83	8.99
Control	PDB	7.41	0.075	7.49

Table (3.4) Percent mass yields were calculated for the time course fractions listed in Table 3.1, including a total yield of the combined Aq and Or extracts for each replicate.

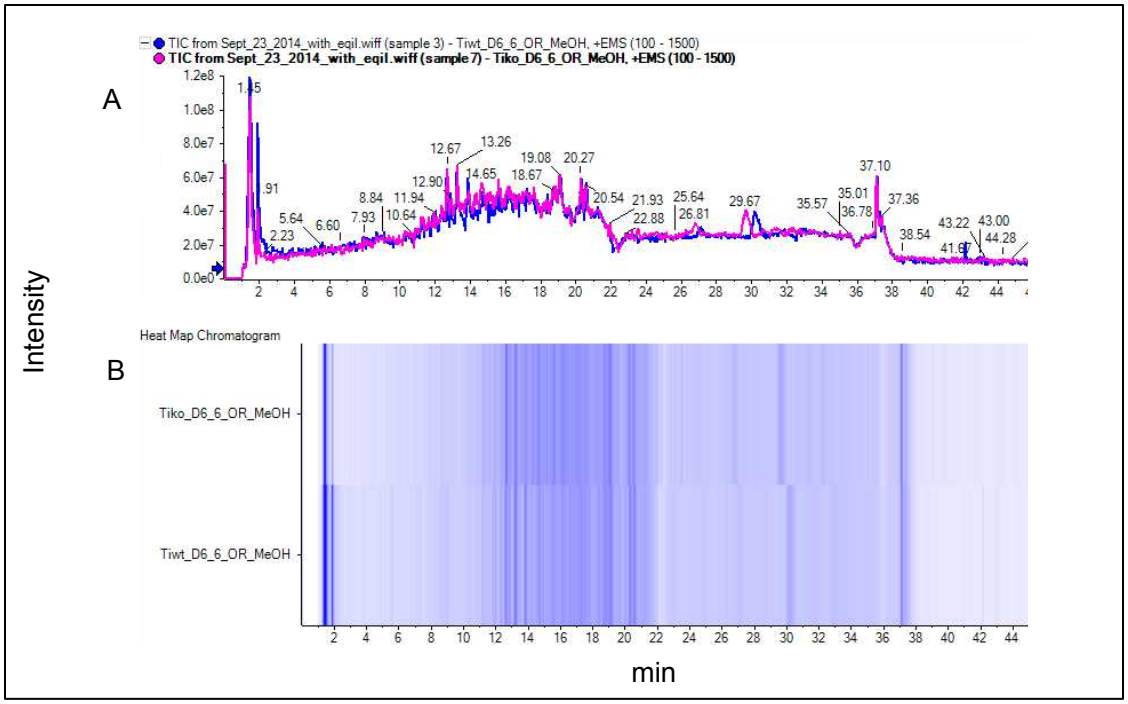

Figure (3.4) LC-MS data for the 100% MeOH fractions of *T. inflatum* extracts grown in PDB displaying similar mass spectrum profiles. A) TIC of TiKO-D6-6-OR-MeOH and TiWT-D6-6-OR-MeOH. B) Heat map of TiKO-D6-6-OR-MeOH and TiWT-D6-6-OR-MeOH displaying similar metabolites between the WT and KO. Blue bands depict the TIC in 2D.

Loss in reproducibility of CsA production by WT *T. inflatum* grown in PDB medium

LC-MS/MS analysis of the 100% MeOH SPE fraction from the organic extract of *T. inflatum* grown in PDB in 2013 (Ti-8044-PDB-M) resulted in greater secondary metabolite production than other selected media. However, new cultures of *T. inflatum* in PDB did not recapitulate our previous results. There was a complete loss of the production of cyclosporins and putative peptaibols in the wild-type *T. inflatum* grown in PDB. Figure 3.5 illustrates the absence of CsA in the *T. inflatum* extracts by contrasting the extracted ion count (XIC) profiles of the LC-MS data for Ti-8044-PDB-M (original sample generated in 2013), TiWT-PDB-Or-MeOH and TiKO-PDB-Or-MeOH. Ions extracted pertaining to cyclosporin A are *m/z* 1202 ± 1.0, $[M+H]^+$ and double-charged ion *m/2z* 601 ± 1.0, $[M+2H]^{2+}$. Cyclosporin A originally eluted at

7.69-7.80 min and also showed signs of streaking between 10.0-11.5 min in 51% and 60-67% CH_3CN-H_2O, respectively. Since the elution times of cyclosporin A are characteristic of hydrophobicity with possible aggregation, a normal phase (organic) extraction and fractionation protocol was used on fresh cultures of wild-type *T. inflatum* grown in PDB. The LC-MS profile of resulting fractions was more consistent with the original Ti-8044-PDB-M. Figures 3.6 and 3.7 show the recovery of CsA and putative peptaibol production, respectively. However, the culture, extraction and profiling of the *T. inflatum* KO from PDB medium was not repeated using the organic solvent protocol due to time and resource constraints. Instead, analyses of the KO and WT grown in SM medium were pursued.

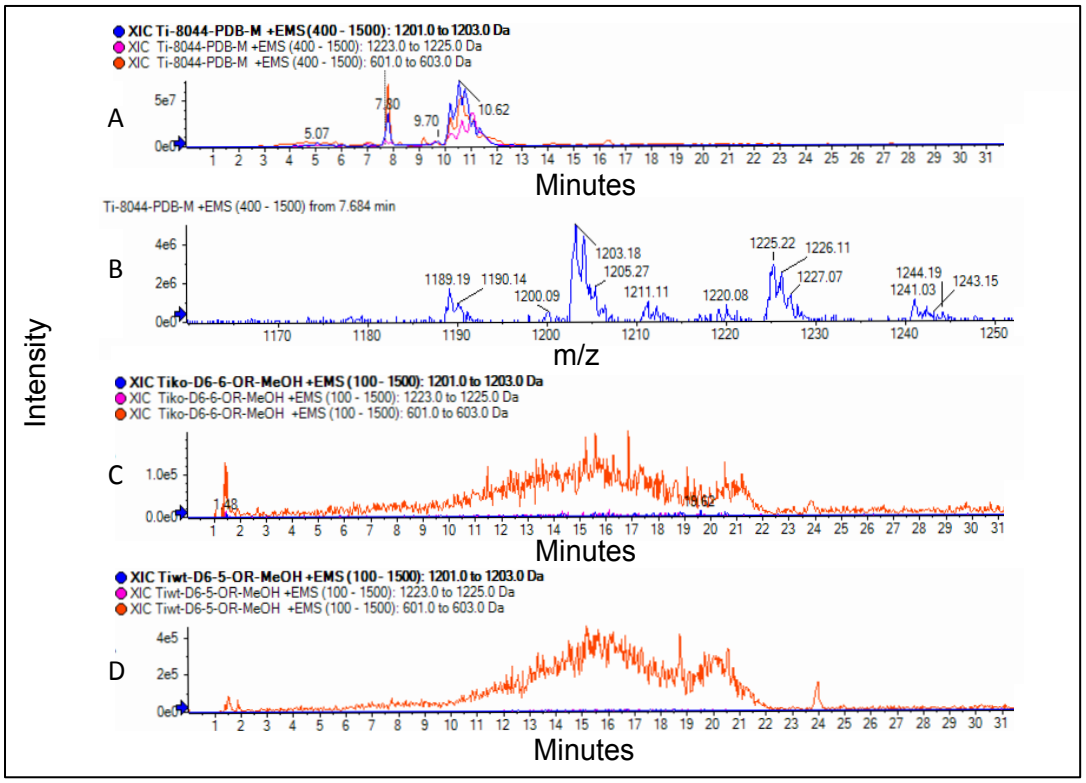

Figure (3.5) LC-MS data for the 100% MeOH fractions of *T. inflatum* extracts grown in PDB: A, B) Ti-8044-PDB-M (original sample), C) TiKO-D6-6-OR-MeOH and D) TiWT-D6-5-OR-MeOH. Traces display the extraction ion count (XIC) for CsA ions, *m/z* 1202 ± 1.0 ($[M+H]^+$) and *m/2z* 601 ± 1.0 ($[M+2H]^{2+}$), which are only present in Ti-8044-PDB-M at RT = 7.80 min and 10-11.50 min.

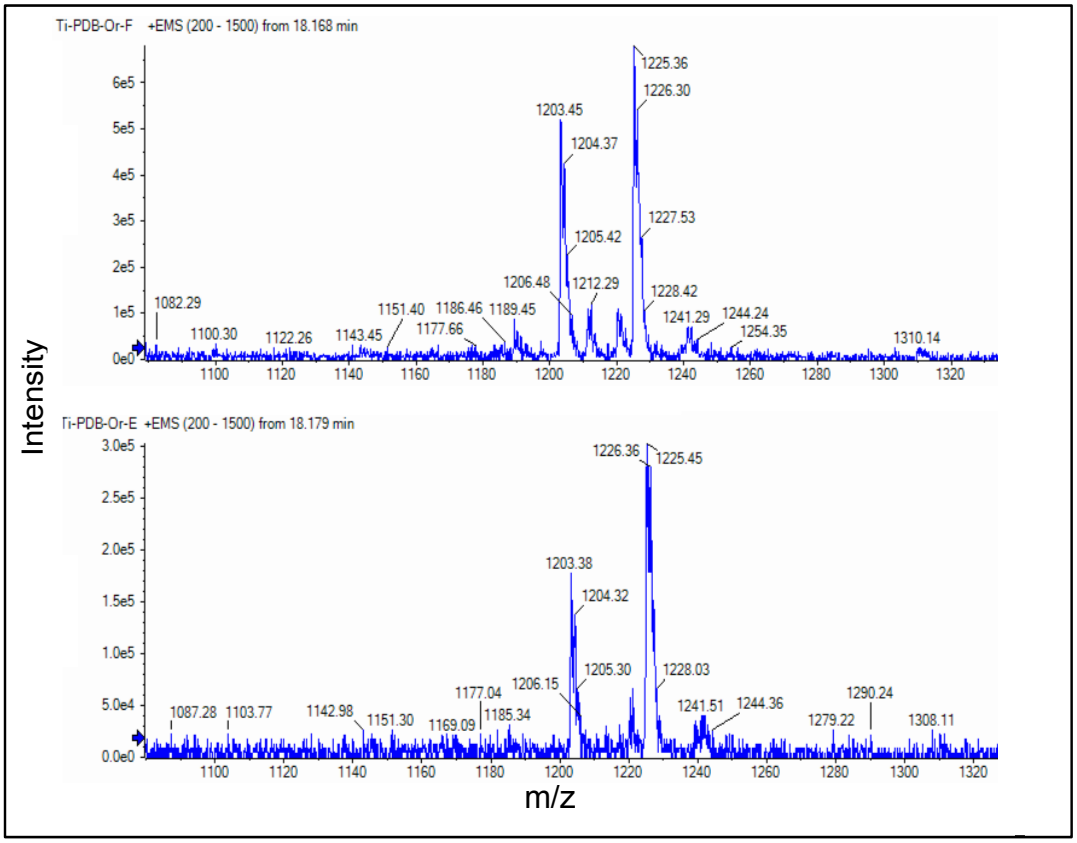

Figure (3.6) TIC chromatographs for normal phase fractions F (100% EtOAc, upper) and E (1:4 hex-EtOAc, lower) from wild-type *T. inflatum* organic extract (as listed in Table 3.3). Traces display cyclosporin A ions *m/z* 1203 ($[M + 2H]^+$) and *m/z* 1225 ($[M+H + Na]^+$)

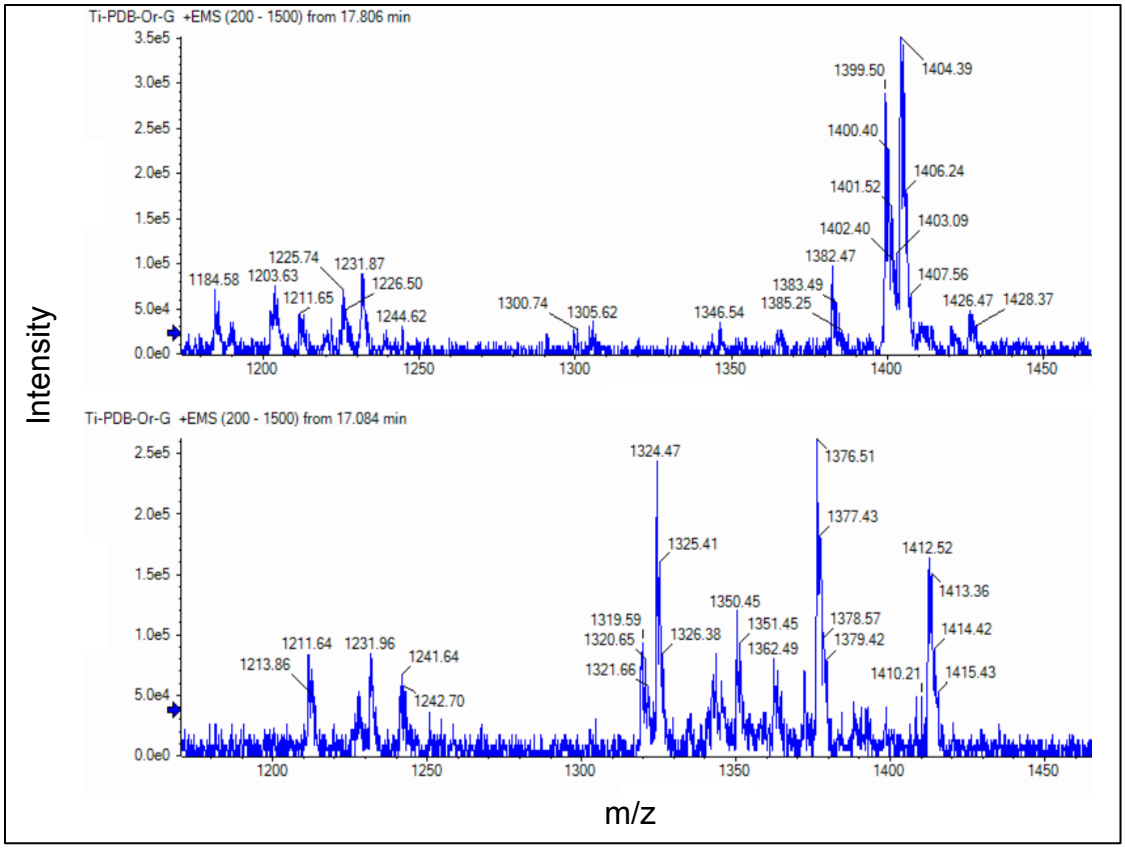

Figure (3.7) TIC chromatographs for normal phase fraction G (1:1 MeOH-EtOAc) from wild-type *T. inflatum* organic extract. Traces display peptaibol ions *m/z* 1403 upper) and *m/z* 1319 and 1376 (lower).

Study of *T. inflatum* Δ*kmt6* versus WT strains grown in SM medium

Given the irregularity of secondary metabolite production and the need for normal phase fractionation of the Ti-PDB organic extract, SM medium was also examined. Organic extracts of WT and KO *T. inflatum* grown in SM were generated and the percent mass yields again showed no significant changes between the WT and KO extracts (Table 3.5). However, the LC-MS data suggests a higher production of metabolites produced from the WT (Figure 3.8B). Dereplication using the online database, informatic search algorithm for natural products (iSNAP) [Ibrahim et al.,

2012] [Steinbeck et al., 2006], was used to investigate the WT and KO, however identification of metabolites was limited due to the low-resolution mass spectrometry data that was acquired. Although the database did not identify the putative peptaibols, iSNAP was able to identify CsA in the WT. iSNAP enables for the identification of compounds through a predictive comparison of fragmentation patterns of unknown samples to those of known natural products in its database. However, this may be very difficult for peptides because of the sequence similarities within the fragmentation patterns. For further analysis the WT underwent hydrolysis and methylation with TMS-diazomethane in order to determine whether the higher order masses could be a cyclic (depsipeptide) or linear in nature and thus provide further support for the hypothesis that they were peptaibols. After the hydrolysis and methylation experiments, the LC-MS data showed little to no signs of the higher masses that are associated to the putative peptaibol. This may suggest that insufficient amounts of material were ascertained through the reactions and therefore the same chemistry may need to be performed on larger amounts of material.

Replicates	*T. inflatum* in SM	Or. Extract % Yield
1	TiWT	2.17
	TiKO	2.36
2	TiWT	1.47
	TiKO	2.19

Table (3.5) Percent organic extract yields for *T. inflatum* grown in SM. Percent yields show no significant changes in mass between the WT and KO extracts.

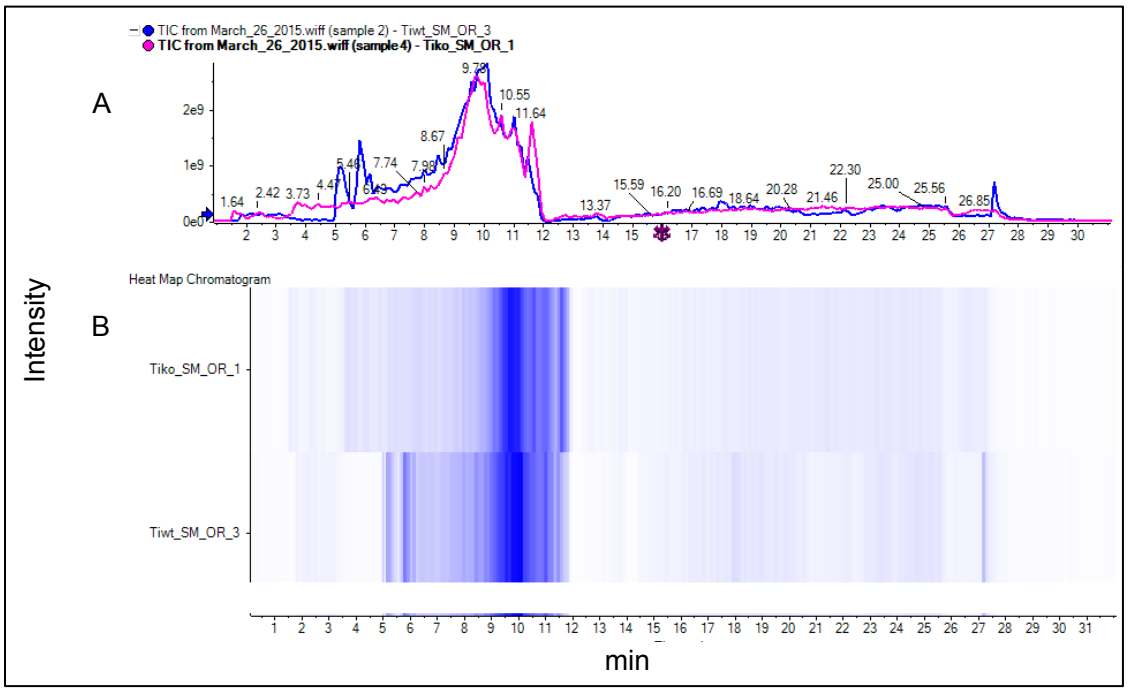

Figure (3.8) LC-MS data for the 100% MeOH fractions of KO and WT extracts grown in SM. A) TIC of TiKO-SM-OR-1 and TiWT-SM-OR-3 B) Heat map of TiKO-SM-OR-1 and TiWT-SM-OR-3 displaying the differences between the metabolites produced between the WT and KO. Blue bands depict the TIC in 2D.

Loss of CsA in *T. inflatum* Δ*kmt6* strain grown in SM medium

T. inflatum is well-known to produce CsA in large quantities, as well as several of its analogues.[Borel, 1997][Bushley et al., 2013] LC-MS/MS profiling of extracts of the KO strain showed no CsA production, in contrast to the WT *T. inflatum* extracts. Figure 3.9 compares the CsA extracted ion count (XIC) from the LC-MS data for TiKO-SM-Or-MeOH (Figure 3.9A) and TiWT-SM-Or-MeOH (Figure 3.9B), which were each generated and analyzed in duplicate. This suggests that the *kmt6* gene homolog may be involved in regulation of CsA production. Further experiments to investigate this hypothesis could make use of transcriptomics to detect the

derepression of *simA*, the gene that encodes the NRPS responsible for the biosynthesis of CsA.

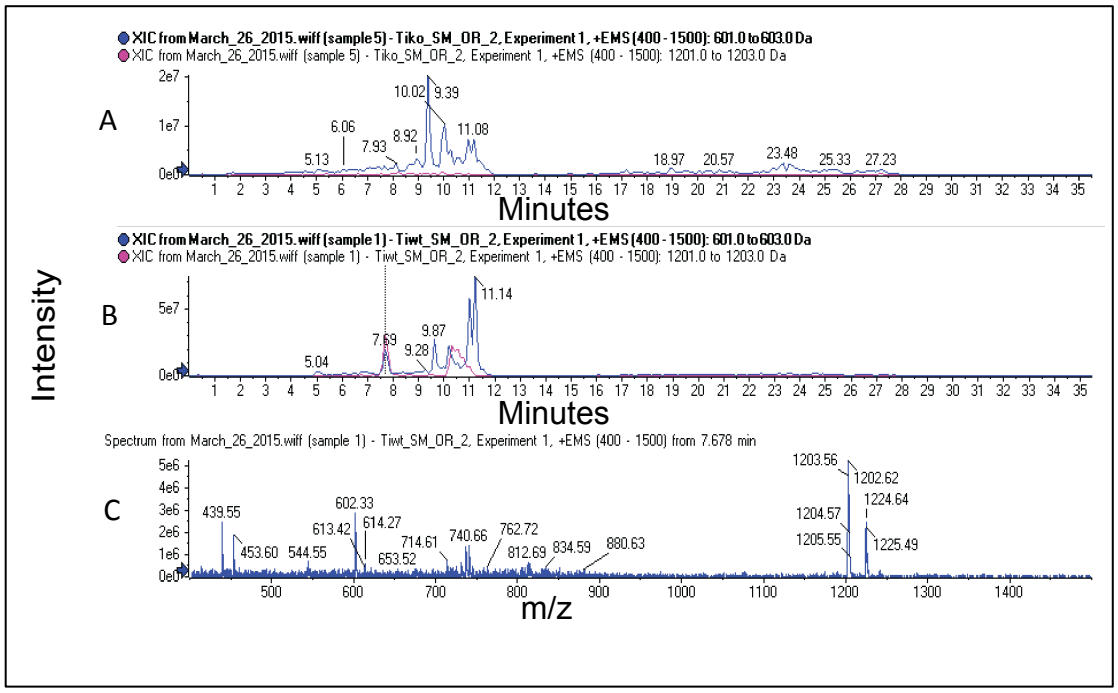

Figure (3.9) LC-MS data for the 100% MeOH SPE fractions from KO and WT *T. inflatum* grown in SM media. A) CsA XIC profiles (for *m/z* 1202 ± 1.0 and 601 ± 1.0) of the KO fraction and B) the WT fraction. C) The WT-derived fraction shows both ions corresponding to CsA at RT = 7.69 min while the KO-derived fraction lacks CsA ions.

Preliminary testing of *T. inflatum* extracts for growth inhibition of *Neisseria gonorrhoeae*

The gram-negative bacterium *Neisseria gonorrhoeae*, also known as gonococcus (GC), is an exclusively human pathogen responsible for the sexually-transmitted infection (STI) gonorrhea. According to the World Health Organization, infection occurs via the mucous membranes of reproductive systems in women and men currently resulting in over 88 million cases of infection worldwide every year.[Organization, 2014] GC causes epididymitis in men and pelvic inflammatory diseases in women, which may

lead to complications such as infertility and ectopic pregnancy.[Edwards et al., 2004] Additionally, GC is associated with human immunodeficiency virus (HIV) infections.[Fleming et al., 1999] [Galvinet al., 2004] Due to GC resistance to previous antibiotic treatments, such as penicillin, erythromycin, tetracycline, and ciprofloxin, the current treatment is a combination of the antibiotics cephalosporin and azithromycin.[Barbee et al., 2013] However, the potential for development of resistance to the latter antibiotics, and the fact that no other clinically viable antibiotics are available is a cause for grave concern.[Rice, 2015] As such, there is an urgent need to find alternative treatments for GC infections.

As proof of concept of the potential for fungal extracts to contains bioactive molecules against GC, the extracts from WT and KO strains of *T. inflatum* grown in PDB were tested in an anti-GC assay performed in the Sikora Lab. The WT extract inhibited the growth of GC throughout the range of concentrations tested (0.5 and 5.0 μg/μL), Figure 3.10. It is very possible that the cyclosporins caused this effect due to high cytotoxicity, although further investigation is needed to confirm this. Interestingly, the organic and aqueous extracts of the KO strain appeared to produce a gradual increase in GC growth over the four time points (0, 3, 6 and 9 h) of the assay.

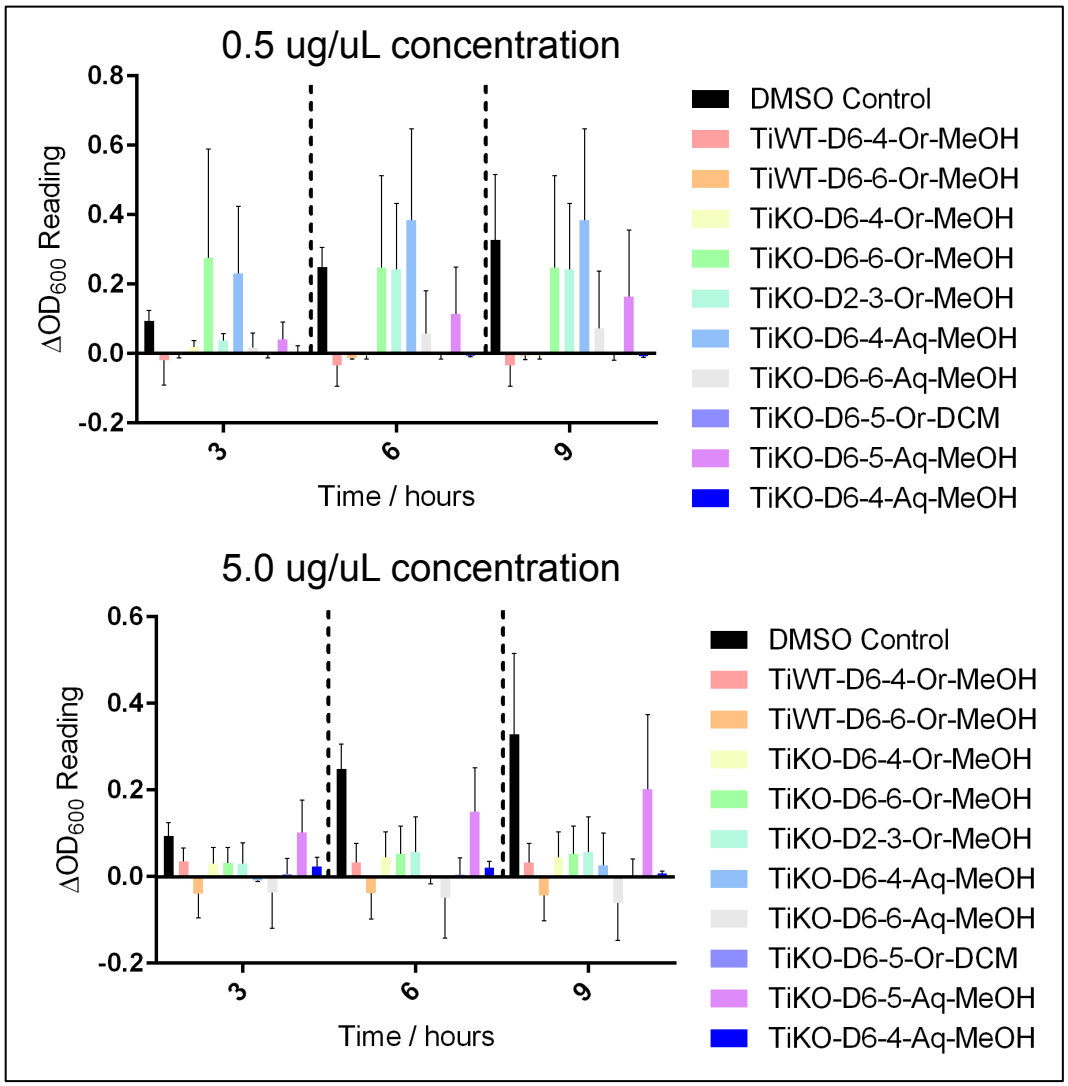

Figure (3.10) Graphs of GC growth (measured by OD_{600}) in the presence of *T. inflatum* extracts, monitored over 9 hours. Extracts of the KO and WT *T. inflatum* grown in PDB were screened at 0.5 and 5.0 μg/μL.

Typically natural product extracts contain a multitude of compounds and further fractionation of the crude mixture is required to pinpoint the compound responsible for the activity. To examine whether a bioassay-guided fractionation strategy could be applied to these fungal extracts, TiKO-D6-Or-MeOH was subjected to HPLC to yield four broad time points (F1, F2, F3, F4), of which F1 and F2 were further separated

into four semi-pure peaks/bands (F1-A, F2-A, F2-B, F2-C), Figure 3.11. All except one fraction (F2-C) exhibited significant GC inhibition, suggesting multiple active compounds (Figure 3.12). Interestingly, F2-C increased GC growth that surpassed the DMSO control. Fraction F2-A resulted in slight growth after three hours but decreased GC growth over nine hours. Fraction F3 produced only slight activity, with increasing GC growth over the hours, while F1 and F1-A resulted in stalled GC growth (acting as bacteriostatic agents). Although the crude TiKO-D6-6-MeOH fraction initially showed relatively little activity, especially at the low tested concentration, the resulting HPLC fractions were found to be significantly active against GC. This result illustrates the challenges of testing very crude mixtures in which all components may not be equally exposed to the test organism in significant titers, and supports the early generation of HPLC peak libraries for testing in relatively high throughput microtiter biological assays. The results also suggest the potential for discovery of *T. inflatum* metabolites that inhibit GC.

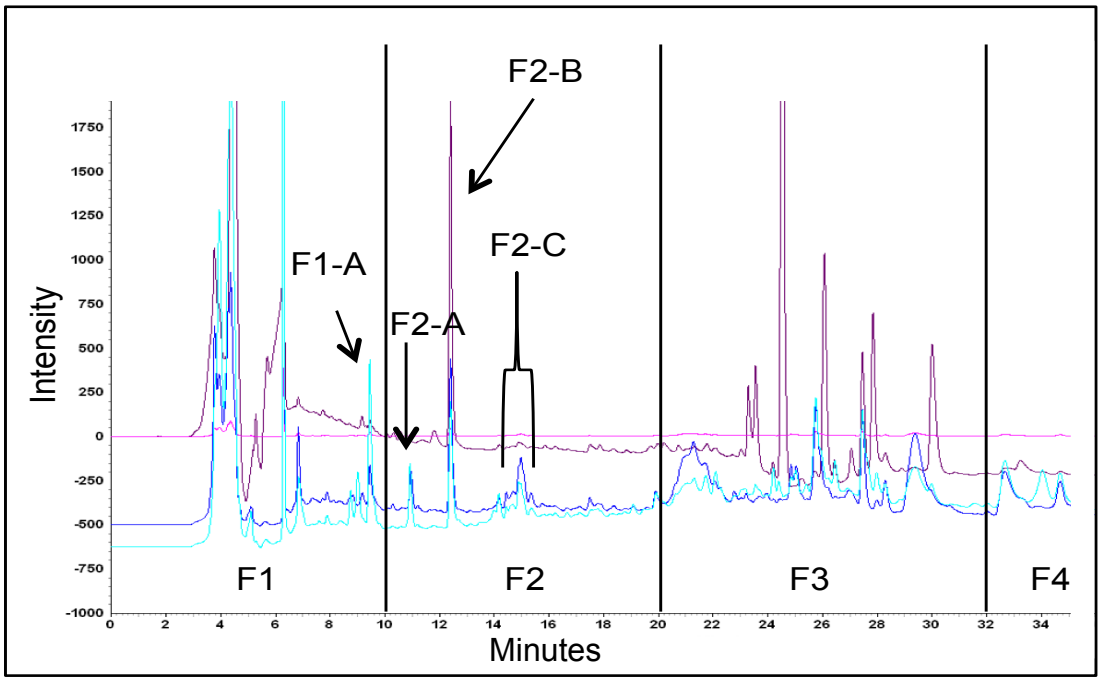

Figure (3.11) HPLC trace for the 100% MeOH SPE fraction from *T. inflatum* KO grown in PDB (TiKO-D6-6-Or-MeOH). Broad time points F1, F2, F3, F4 were collected, as well as the labeled peaks F1-A, F2-A, F2-B and F2-C. Fractions were collected using UV detection at 190 (purple), 257 (cyan), 274 (pink) and 280 nm (blue).

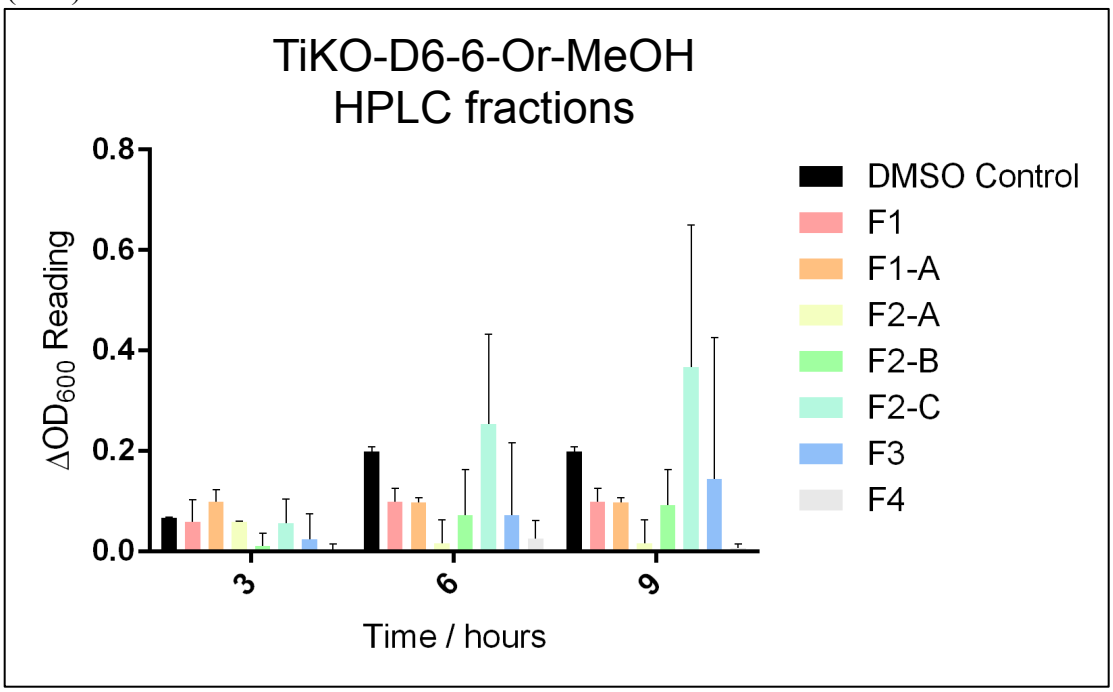

Figure (3.12) HPLC fractions from TiKO–D6-6-Or-MeOH were screened in a GC inhibition assay performed in the Sikora Lab. Fractions F1, F1-A, F2-B, F2-C, F3 displayed some degree of GC inhibition, with fractions F2-A and F4 having the activity.

Conclusion

Comparative metabolomic profiling using LC-MS/MS was undertaken to determine whether a phenotypic change, manifested in altered secondary metabolite production, could be detected for a mutant strain of *T. inflatum*, in which a homolog of the *kmt6* methyltransferase gene was knocked out. The KMT6 methyltransferase is associated with secondary metabolite expression in *Fusarium* species. A time course study was performed in which triplicate cultures of wild-type *T.inflatum* NRRL 8044 and the *kmt6* homolog knockout strain were harvested on days 2, 6 and 10 for extraction, fractionation and comparison of their LC-MS/MS profiles. Initially the two strains were cultured in PDB medium. However, the LC-MS profiles did not reproduce the results of a 2013 study in which CsA and putative peptaibols were obtained from aqueous extracts of *T. inflatum* grown in PDB medium. For this reason, the KO and WT *T. inflatum* strains were grown in duplicate in SM medium instead. Somewhat disappointingly, no increased production of multiple secondary metabolites could be detected. Instead, LC-MS profiling of the resulting extracts revealed the production of CsA by WT cultures, but not by the KO *T. inflatum* strain. This suggests that the *T. inflatum* homolog of the KMT6 methyltransferase is a regulator of the NRPS gene for CsA production, *simA*. Further work will focus on elucidating whether this methyltransferase gene is associated with regulating other secondary metabolites, and also whether manipulation of this gene can result in expression of compounds that are not expressed in the wild type strain. In preliminary biological assays, extracts from *T. inflatum* and the *kmt6* KO strain exhibited inhibitory effects on the growth of *N.*

gonhorreaea suggesting multiple potent compounds distributed in several fractions. These results also warrant further work, including bioassay-guided fractionation of bulk extracts from *T. inflatum*.

BIBLIOGRAPHY

Albright, J. C., Henke, M. T., Soukup, A. A., McClure, R. A., Thomson, R. J., Keller, N. P., & Kelleher, N. L. (2015). Large-Scale Metabolomics Reveals a Complex Response of *Aspergillus nidulans* to Epigenetic Perturbation. *ACS Chem. Biol.*, *10*(6), 1535–41.

Bandani, A. R., Khambay, B. P. S., Faull, J. L., Newton, R., Deadman, M., & Butt, T. M. (2000). Production of efrapeptins by *Tolypocladium* species and evaluation of their insecticidal and antimicrobial properties. *Mycol. Res.*, *104*(5), 537–544.

Barbee, L. A., Kerani, R. P., Dombrowski, J. C., Soge, O. O., & Golden, M. R. (2013). A retrospective comparative study of 2-drug oral and intramuscular cephalosporin treatment regimens for pharyngeal gonorrhea. *Clin. Infect. Dis.*, *56*(11), 1539–45.

Barron, G. L. (2011). Fungal parasites of rotifers: a new *Tolypocladium* with underwater conidiation. *Can. J. Bot.*, *58*(4), 439–442.

Bodley, J. W., Zieve, F. J., Lin, L., & Zieve, S. T. (1969). Formation of the ribosome-G factor-GDP complex in the presence of fusidic acid. *Biochem. Biophys. Res. Commun.*, *37*(3), 437–443.

Bok, J. W., & Keller, N. P. (2004). LaeA, a regulator of secondary metabolism in *Aspergillus* spp. *Eukaryot. Cell*, *3*(2), 527–535.

Borel, J.-F. (1997). La ciclosporine en immunologie. *BioDrugs*, *8*(Supplement 1), 1–3.

Brakhage, A. A. (2013). Regulation of fungal secondary metabolism. *Nat. Rev. Microbiol.*, *11*(1), 21–32.

Bushley, K. E., Raja, R., Jaiswal, P., Cumbie, J. S., Nonogaki, M., Boyd, A. E., Spatafora, J. W. (2013). The Genome of *Tolypocladium inflatum*: Evolution, Organization, and Expression of the Cyclosporin Biosynthetic Gene Cluster. *PLoS Genet.*, *9*(6).

Chun, G.-T., & Agathos, S. N. (1989). Immobilization of *Tolypocladium inflatum* spores into porous celite beads for cyclosporine production. *J. Biotechnol.*, *9*(4), 237–254.

Connolly, L. R., Smith, K. M., & Freitag, M. (2013). The *Fusarium graminearum* histone H3 K27 methyltransferase KMT6 regulates development and expression of secondary metabolite gene clusters. *PLoS Genet.*, *9*(10), e1003916.

De Girolamo, A., Lattanzio, V. M. T., Schena, R., Visconti, A., & Pascale, M. (2014). Use of liquid chromatography-high-resolution mass spectrometry for isolation and characterization of hydrolyzed fumonisins and relevant analysis in maize-based products. *J. Mass Spectrom.*, *49*(4), 297–305.

Degenkolb, T., Kirschbaum, J., & Brückner, H. (2007). New sequences, constituents, and producers of peptaibiotics: An updated review. *Chem. Biodivers.*

Edwards, J. L., & Apicella, M. A. (2004). The molecular mechanisms used by Neisseria gonorrhoeae to initiate infection differ between men and women. *Clin. Microbiol. Rev.*

El-Elimat, T., Figueroa, M., Ehrmann, B. M., Cech, N. B., Pearce, C. J., & Oberlies, N. H. (2013). High-resolution MS, MS/MS, and UV database of fungal secondary metabolites as a dereplication protocol for bioactive natural products. *J. Nat. Prod.*, *76*(9), 1709–16.

Endo, A., Kuroda, M., & Tsujita, Y. (1976). ML-236A, ML-236B, and ML-236C, new inhibitors of cholesterogenesis produced by *Penicillium citrinium*. *J. Antibiot. (Tokyo).*, *29*(12), 1346–1348.

Evidente, A., Kornienko, A., Cimmino, A., Andolfi, A., Lefranc, F., Mathieu, V., & Kiss, R. (2014). Fungal metabolites with anticancer activity. *Nat. Prod. Rep.*, *31*(5), 617–27.

Feher, M., & Schmidt, J. M. (2003). Property distributions: Differences between drugs, natural products, and molecules from combinatorial chemistry. *J. Chem. Inf. Comput. Sci.*, *43*(1), 218–227.

Fleming, D. T., & Wasserheit, J. N. (1999). From epidemiological synergy to public health policy and practice: the contribution of other sexually transmitted diseases to sexual transmission of HIV infection. *Sex. Transm. Infect.*, *75*(1), 3–17.

Fukuda, T., Sudoh, Y., Tsuchiya, Y., Okuda, T., Matsuura, N., Motojima, A., … Igarashi, Y. (2015). Tolypoalbin, a new tetramic acid from *Tolypocladium album* TAMA 479. *J. Antibiot. (Tokyo).*

Galvin, S. R., & Cohen, M. S. (2004). The role of sexually transmitted diseases in HIV transmission. *Nat. Rev. Microbiol.*, *2*(1), 33–42.

Gelderblom, W. C. A., Jaskiewicz, K., Marasas, W. F. O., Thiel, P. G., Horak, R. M., Vleggaar, R., & Kriek, N. P. J. (1988). Fumonisins - novel mycotoxins with cancer-promoting activity produced by *Fusarium moniliforme*. *Appl. Environ. Microbiol.*, *54*(7), 1806–1811.

Georgopoulos, K. (2002). Haematopoietic cell-fate decisions, chromatin regulation and ikaros. *Nat. Rev. Immunol.*, *2*(3), 162–74.

Godtfredsen, W. O., Jahnsen, S., Lorck, H., Roholt, K., & Tybring, L. (1962). Fusidic acid: a new antibiotic. *Nature*, *193*, 987.

Gupta, S., Krasnoff, S. B., Roberts, D. W., Renwick, J. A. A., Brinen, L. S., & Clardy, J. (1992). Structure of efrapeptins from the fungus *Tolypocladium niveum*: peptide inhibitors of mitochondrial ATPase. *J. Org. Chem.*, *57*(8), 2306–2313.

Howell, C. R. (2007). Understanding the Mechanisms Employed by *Trichoderma* virens to Effect Biological Control of Cotton Diseases., *96*(2), 178

Huang, H., Wang, F., Luo, M., Chen, Y., Song, Y., Zhang, W., … Ju, J. (2012). Halogenated anthraquinones from the marine-derived fungus *Aspergillus* sp. SCSIO F063. *J. Nat. Prod.*, *75*(7), 1346–52.

Ibrahim, A., Yang, L., Johnston, C., Liu, X., Ma, B., & Magarvey, N. A. (2012). Dereplicating nonribosomal peptides using an informatic search algorithm for natural products (iSNAP) discovery. *Proc. Natl. Acad. Sci. U. S. A.*, *109*(47), 19196–201.

Jackson, C. G., Linnett, P. E., Beechey, R. B., & Henderson, P. J. (1979). Purification and preliminary structural analysis of the efrapeptins, a group of antibiotics that inhibit the mitochondrial adenosine triphosphatase [proceedings]. *Biochem. Soc. Trans.*, *7*(1), 224–6.

Jin, L., & Harrison, S. C. (2002). Crystal structure of human calcineurin complexed with cyclosporin A and human cyclophilin. *Proc. Natl. Acad. Sci. U. S. A.*, *99*(21), 13522–6.

Kanasaki, R., Kobayashi, M., Fujine, K., Sato, I., Hashimoto, M., Takase, S., Hori, Y. (2006). FR227673 and FR190293, novel antifungal lipopeptides from *Chalara* sp. No. 22210 and *Tolypocladium parasiticum* No. 16616. *J. Antibiot. (Tokyo).*, *59*(3), 158–67.

Keller, N. P., Turner, G., & Bennett, J. W. (2005). Fungal secondary metabolism - from biochemistry to genomics. *Nat. Rev. Microbiol.*, *3*(12), 937–47.

Kellogg, D. S. J., Peacock, W. L. J., Deacon, W. E., Brown, L., & Pirkle, C. I. (1963). *NEISSERIA GONORRHOEAE* I.: Virulence Genetically Linked to Clonal Variation. *J. Bacteriol.*, *85*(6), 1274–1279.

Kepler, R. M., Sung, G.-H., Ban, S., Nakagiri, A., Chen, M.-J., Huang, B., Spatafora, J. W. (2012). New teleomorph combinations in the entomopathogenic genus *Metacordyceps*. *Mycologia*, *104*(1), 182–97.

Kim, H., & Woloshuk, C. P. (2008). Role of AREA, a regulator of nitrogen metabolism, during colonization of maize kernels and fumonisin biosynthesis in *Fusarium verticillioides*. *Fungal Genet. Biol.*, *45*(6), 947–953.

Kimanya, M. E., De Meulenaer, B., Roberfroid, D., Lachat, C., & Kolsteren, P. (2010). Fumonisin exposure through maize in complementary foods is inversely associated with linear growth of infants in Tanzania. *Mol. Nutr. Food Res.*, *54*(11), 1659–1667.

Krasnoff, S. B., & Gupta, S. (1992). Efrapeptin production by *Tolypocladium* fungi (Deuteromycotina: Hyphomycetes): Intra- and interspecific variation. *J. Chem. Ecol.*, *18*(10), 1727–1741.

Krasnoff, S. B., Gupta, S., Leger, R. J. S., Renwick, J. A. A., & Roberts, D. W. (1991). Antifungal and insecticidal properties of the efrapeptins: Metabolites of the fungus *Tolypocladium niveum*. *J. Invertebr. Pathol.*, *58*(2), 180-188.

Krug, D., & Müller, R. (2014). Secondary metabolomics: the impact of mass spectrometry-based approaches on the discovery and characterization of microbial natural products. *Nat. Prod. Rep.*, *31*(6), 768–83.

Li, C., Mi, T., Conti, G. O., Yu, Q., Wen, K., Shen, J., Wang, Z. (2015). Development of a screening fluorescence polarization immunoassay for the simultaneous detection of fumonisins B1 and B2 in maize. *J. Agric. Food Chem.*, *63*(20), 4940–6.

Marasas, W. F. O., Riley, R. T., Hendricks, K. A., Stevens, V. L., Sadler, T. W., Gelineau-van Waes, J., Merrill, A. H. J. (2004). Fumonisins Disrupt Sphingolipid Metabolism, Folate Transport, and Neural Tube Development in Embryo Culture and In Vivo: A Potential Risk Factor for Human Neural Tube Defects among Populations Consuming Fumonisin-Contaminated Maize. *J. Nutr.*, *134*(4), 711–716.

Mogensen, J. M., Møller, K. A., von Freiesleben, P., Labuda, R., Varga, E., Sulyok, M., Nielsen, K. F. (2011). Production of fumonisins B2 and B4 in *Tolypocladium* species. *J. Ind. Microbiol. Biotechnol.*, *38*(9), 1329–35.

Molnár, I., Gibson, D. M., & Krasnoff, S. B. (2010). Secondary metabolites from entomopathogenic Hypocrealean fungi. *Nat. Prod. Rep.*, *27*(9), 1241–75.

Musser, S. M., & Plattner, R. D. (1997). Fumonisin Composition in Cultures of *Fusarium moniliforme, Fusarium proliferatum, and Fusarium nygami*. *J. Agric. Food Chem.*, *45*(4), 1169–1173.

Newman, D. J., & Cragg, G. M. (2012). Natural products as sources of new drugs over the 30 years from 1981 to 2010. *J. Nat. Prod.*

Nützmann, H.-W., Reyes-Dominguez, Y., Scherlach, K., Schroeckh, V., Horn, F., Gacek, A., Brakhage, A. A. (2011). Bacteria-induced natural product formation in the fungus *Aspergillus nidulans* requires Saga/Ada-mediated histone acetylation. *Proc. Natl. Acad. Sci. U. S. A.*, *108*(34), 14282–7.

O'Keefe, S. J., Tamura, J., Kincaid, R. L., Tocci, M. J., & O'Neill, E. A. (1992). FK-506- and CsA-sensitive activation of the interleukin-2 promoter by calcineurin. *Nature*, *357*(6380), 692–4.

Organization, W. H. (2014). Report on global sexually transmitted infection surveillance 2013. World Health Organization.

Oxford, A. E., Raistrick, H., & Simonart, P. (1939). Studies in the biochemistry of micro-organisms: Griseofulvin, C(17)H(17)O(6)Cl, a metabolic product of *Penicillium griseo-fulvum* Dierckx. *Biochem. J.*, *33*(2), 240–8.

Pflügl, G., Kallen, J., Schirmer, T., Jansonius, J. N., Zurini, M. G., & Walkinshaw, M. D. (1993). X-ray structure of a decameric cyclophilin-cyclosporin crystal complex. *Nature*, *361*(6407), 91–4.

Quandt, C. A., Kepler, R. M., Gams, W., Araújo, J. P. M., Ban, S., Evans, H. C., Spatafora, J. W. (2014). Phylogenetic-based nomenclatural proposals for Ophiocordycipitaceae (Hypocreales) with new combinations in *Tolypocladium*. *IMA Fungus*, *5*(1), 121–34.

Reyes-Dominguez, Y., Bok, J. W., Berger, H., Shwab, E. K., Basheer, A., Gallmetzer, A., Strauss, J. (2010). Heterochromatic marks are associated with the repression of secondary metabolism clusters in *Aspergillus nidulans*. *Mol. Microbiol.*, *76*(6), 1376–86.

Rice, L. B. (2015). Will use of combination cephalosporin/azithromycin therapy forestall resistance to cephalosporins in *Neisseria gonorrhoeae* ? *Sex. Transm. Infect.*, *91*(4), 238–40.

Savile, D. B. O. (1968). Possible interrelationships between fungal groups. *Fungi. An Adv. Treatise. Acad. Press. New York*, 649–675.

Shigemori, H., Wakuri, S., Yazawa, K., Nakamura, T., Sasaki, T., & Kobayashi, J. (1991). Fellutamides A and B, cytotoxic peptides from a marine fish-possessing fungus *Penicillium fellutanum*. *Tetrahedron*, *47*(40), 8529–8534.

Shilatifard, A. (2006). Chromatin modifications by methylation and ubiquitination: implications in the regulation of gene expression. *Annu. Rev. Biochem.*, *75*, 243–69.

Spatafora, J. W., Sung, G.-H., Sung, J.-M., Hywel-Jones, N. L., & White, J. F. (2007). Phylogenetic evidence for an animal pathogen origin of ergot and the grass endophytes. *Mol. Ecol.*, *16*(8), 1701–11.

Spence, J. M., Wright, L., & Clark, V. L. (2008). Laboratory maintenance of *Neisseria gonorrhoeae. Curr. Protoc. Microbiol.*, *Chapter 4*, Unit 4A.1.

Sriwati, R., Melnick, R. L., Muarif, R., Strem, M. D., Samuels, G. J., & Bailey, B. A. (2015). *Trichoderma* from Aceh Sumatra reduce Phytophthora lesions on pods and cacao seedlings. *Biol. Control*, *89*, 33–41.

Steinbeck, C., Hoppe, C., Kuhn, S., Floris, M., Guha, R., & Willighagen, E. (2006). Recent Developments of the Chemistry Development Kit (CDK) - An Open-Source Java Library for Chemo- and Bioinformatics. *Curr. Pharm. Des.*, *12*(17), 2111–2120.

Sung, G.-H., Hywel-Jones, N. L., Sung, J.-M., Luangsa-Ard, J. J., Shrestha, B., & Spatafora, J. W. (2007). Phylogenetic classification of Cordyceps and the clavicipitaceous fungi. *Stud. Mycol.*, *57*, 5–59.

Sung, G.-H., Poinar, G. O., & Spatafora, J. W. (2008). The oldest fossil evidence of animal parasitism by fungi supports a Cretaceous diversification of fungal-arthropod symbioses. *Mol. Phylogenet. Evol.*, *49*(2), 495–502.

Sung, G.-H., Sung, J.-M., Hywel-Jones, N. L., & Spatafora, J. W. (2007). A multi-gene phylogeny of Clavicipitaceae (Ascomycota, Fungi): identification of localized incongruence using a combinational bootstrap approach. *Mol. Phylogenet. Evol.*, *44*(3), 1204–23.

Tsantrizos, Y. S., Pischos, S., & Sauriol, F. (1996). Structural Assignment of the Peptide Antibiotic LP237-F8, a Metabolite of *Tolypocladium geodes*. *J. Org. Chem.*, *61*(6), 2118–2121.

Tsantrizos, Y. S., Pischos, S., Sauriol, F., & Widden, P. (1996). Peptaibol metabolites of *Tolypocladium geodes. Can. J. Chem.*, *74*(2), 165–172.

Velkov, T., Horne, J., Scanlon, M. J., Capuano, B., Yuriev, E., & Lawen, A. (2011). Characterization of the N-methyltransferase activities of the multifunctional polypeptide cyclosporin synthetase. *Chem. Biol.*, *18*(4), 464–75.

Weber, G., Schörgendorfer, K., Schneider-Scherzer, E., & Leitner, E. (1994). The peptide synthetase catalyzing cyclosporine production in Tolypocladium niveum is encoded by a giant 45.8-kilobase open reading frame. *Curr. Genet.*, *26*(2), 120–5.

Weber, K., Wehland, J., & Herzog, W. (1976). Griseofulvin interacts with microtubules both in vivo and in vitro. *J. Mol. Biol.*, *102*(4), 817–829.

Weigelt, S., Huber, T., Hofmann, F., Jost, M., Ritzefeld, M., Luy, B., … Sewald, N. (2012). Synthesis and conformational analysis of efrapeptins. *Chemistry*, *18*(2), 478–87.

Yuliana, N. D., Khatib, A., Choi, Y. H., & Verpoorte, R. (2011). Metabolomics for bioactivity assessment of natural products. *Phytother. Res.*, *25*(2), 157–69.